STRANGE BARYON RESONANCES

Chairman	V. Dzhelepov
Rapporteur	N. Samios
Discussion leader	C. Bricman
Secretaries	V. Vinogradov
	V. Flyagin

STRANGE BARYON RESONANCES

N. Samios

Even though experiments on baryon spectroscopy take of the order of a year or more to perform and analyze, and conferences such as this occur at a rate of once a year, it is indeed amazing that some new results are reported at such gatherings. This is due to both the observation of new phenomena as well as the reporting of new numbers on old physics questions. Today I will attempt to summarize for you the experimental situation concerning baryon resonances with strangeness different from zero. As such, my talk will encompass the material presented at this Conference, articles and letters published within the last year, preliminary results presented at the Duke Conference [1], and, where appropriate, some background material to place the subject in proper context. I propose to divide this subject into four sections:

1. Z^* States — Examination of the possible existence of states with baryon number $N = 1$, strangeness $S = +1$ with isospin $I = 0, 1$.
2. Λ, Σ States — Review the multitude of information concerning these properties and existence of such resonances.
3. Ξ States — Discuss the relevant old and new data concerning new states.
4. Particle Systematics — Classification of the more well-established states into SU (3) multiplets as well as an examination of the Regge recurrence of such resonances.

1. Z^* States

As is well known, interest in the existence of such resonances is of extreme importance because they can only be accommodated in either a $\overline{10}$ or 27 representation, while all the well-established bosons are members of 1 or 8 representations and baryon members of 1, 8, or 10 representations. This

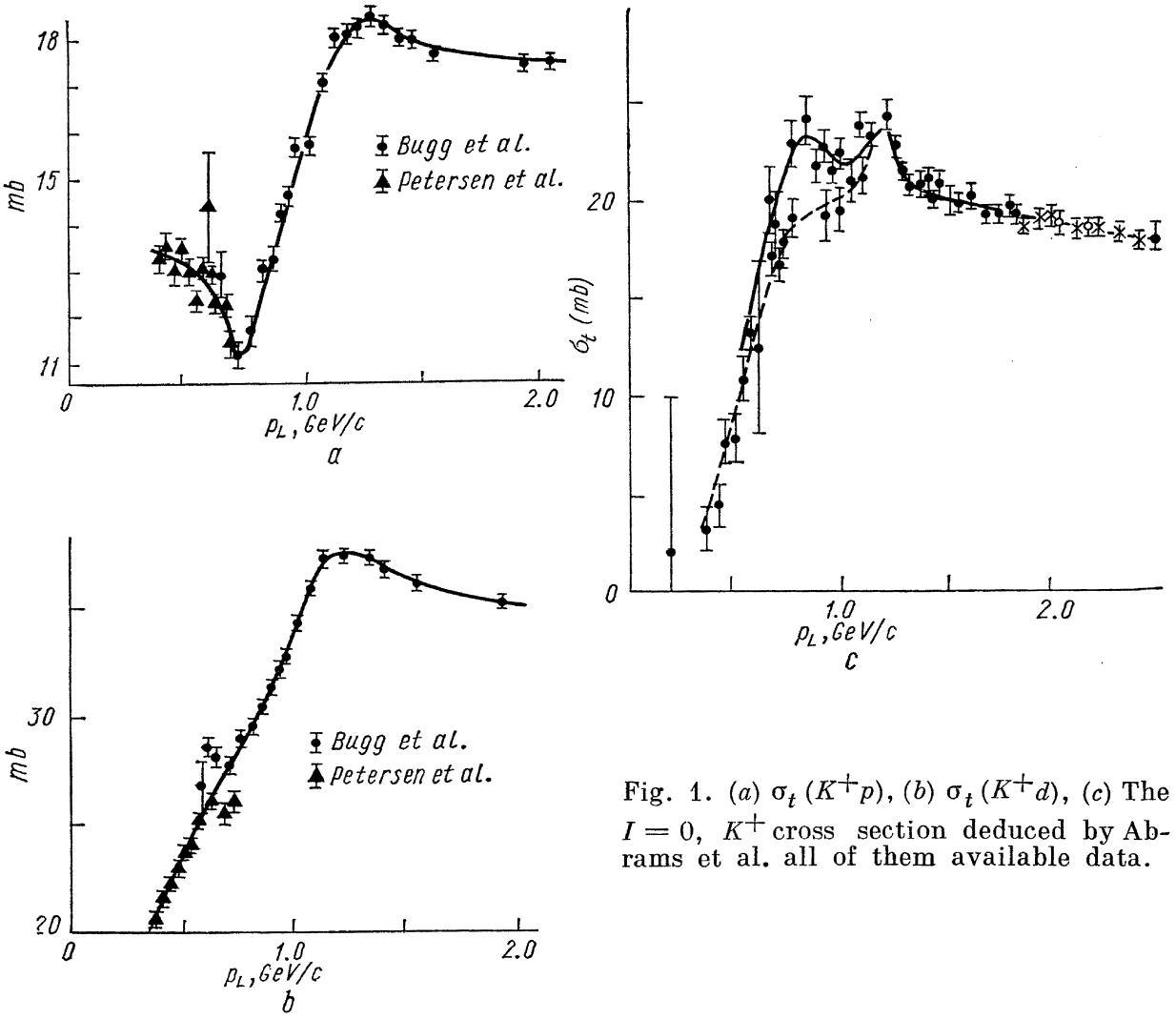

Fig. 1. (*a*) $\sigma_t(K^+p)$, (*b*) $\sigma_t(K^+d)$, (*c*) The $I = 0$, K^+ cross section deduced by Abrams et al. all of them available data.

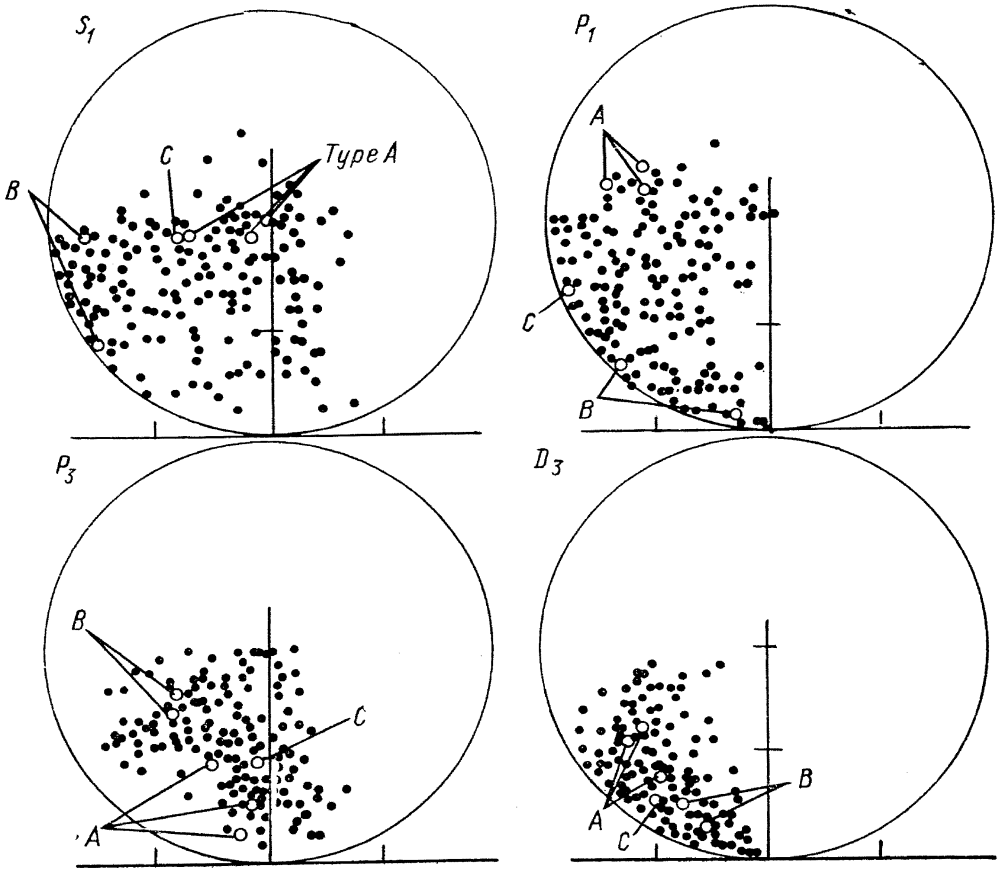

Fig. 2. CERN. $K^+p \to \to K^+p$ at 1.90 *GeV/c*. Argand diagram for S_1-, P_1-, P_3-, and *D*-waves at 1.9 *GeV/c*. 200 phase shift solutions are shown, obtained in 350 random searches.

observation led Gell — Mann [2] and Zweig [3] to propose quarks to account for this limitation. As such, baryons are composed of three quarks, and since the sole strange quark has strangeness $S = -1$, it is not possible to construct an $S = +1$ baryon with such a system. One needs a minimum of four quarks and one antiquark.

The original evidence for a bump in both the $I = 1$ and $I = 0$ states was first presented by Cool et al. [4] as deduced from K^+p and K^+d total cross section measurements. These two states with $M = 1900$ *MeV* and $\Gamma = 250$ *MeV* for the $I = 1$ member and $M = 1870$ *MeV* and $\Gamma = 160$ *MeV* for the $I = 0$ state have since been confirmed by Bugg et al. [5]. The experimental evidence is shown in Fig. 1 where the relevant total cross sections are shown as well as the unfolded $I = 0$ cross sections as deduced by Abrams et al. [6]. The main interest in the Z_1^*

Table I

$I = 1$, $M = 1900$ *MeV*, $\Gamma = 250$ *MeV*
σ_T, σ_l, $d\sigma/d\Omega$ (elastic) and polarization

$d\sigma/d\Omega$ and Polarization Measurements 1.0—2.5 *GeV/c*	
1. CERN (Erne)	
2. Yale (Hughes)	
3. ANL — Maryland — Northwestern — NAL (Yokosawa)	Energy Independent
$d\sigma/d\Omega$ 0.9—2.3 *GeV/c*	
1. University College London — Rutherford (Duff)	
2. Bologna — Glasgow — Roma — Trieste (Giacomelli)	Energy Dependent
Inelastic Channels	
1. Berkeley (Bland et al., Goldhaber)	
2. BGRT (Giacomelli)	
3. Cal Tech. (Gomez)	

past year has been focussed on the $I = 1$ bump. This has involved measurements of the differential elastic cross sections, proton polarizations, and partial cross sections in the energy range from 0.9—2.5 *GeV/c*. A list of the various contributing groups is displayed in Table I. The experimental agreement among the various groups is excellent, both in the polarization measurements as well as the partial cross sections. The procedure for an amplitude analysis adopted by four of the groups is the energy independent approach, to be contrasted with the energy dependent method of one of the groups. In both cases, all the published data are utilized. In the former approach, one attempts to derive all possible solutions at each energy and then to join them in some smooth fashion by adopting some continuity criterion. In practice one applies this technique first at low energies, where only a few partial waves, for instance S and P waves, occur and then to add higher partial waves D, F, etc. as the energy is increased and as needed. The difficulties with such a procedure are illustrated in Fig. 2, where 200 solutions for the S, P, and D waves are displayed in Argand plots for the 1.90 *GeV/c* K^+p elastic reaction as presented by the CERN group [7]. Nevertheless three groups; Yale [8], Argonne — Maryland — North western — NAL [9], and the previously noted CERN [7] group have found many solutions among which is one that has the properties expected of a resonant wave in the $P_{3/2}$ amplitude, namely counter-clockwise circular motion in an Argand diagram. In Fig. 3 the Yale solution for this $P_{3/2}$ amplitude is shown as well as the Argonne cross section for the same amplitude. In addition the $I = 1$ inelastic cross section, as measured by Goldhaber et al. [10], is also included which shows that the increase in cross section is associated with the K^*N partial cross section. However a study of the contributing partial waves in the $K\Delta$ channel, which also peaks at a similar mass by the same group [11], is inconclusive but includes among its possibilities a highly inelastic $P_{3/2}$ wave which is consistent with that of the above groups. Cross sections for P_3 and D_5 amplitudes from the CERN analysis is shown in Fig. 4, where solution γ appears to be resonant. An examination of the rate of

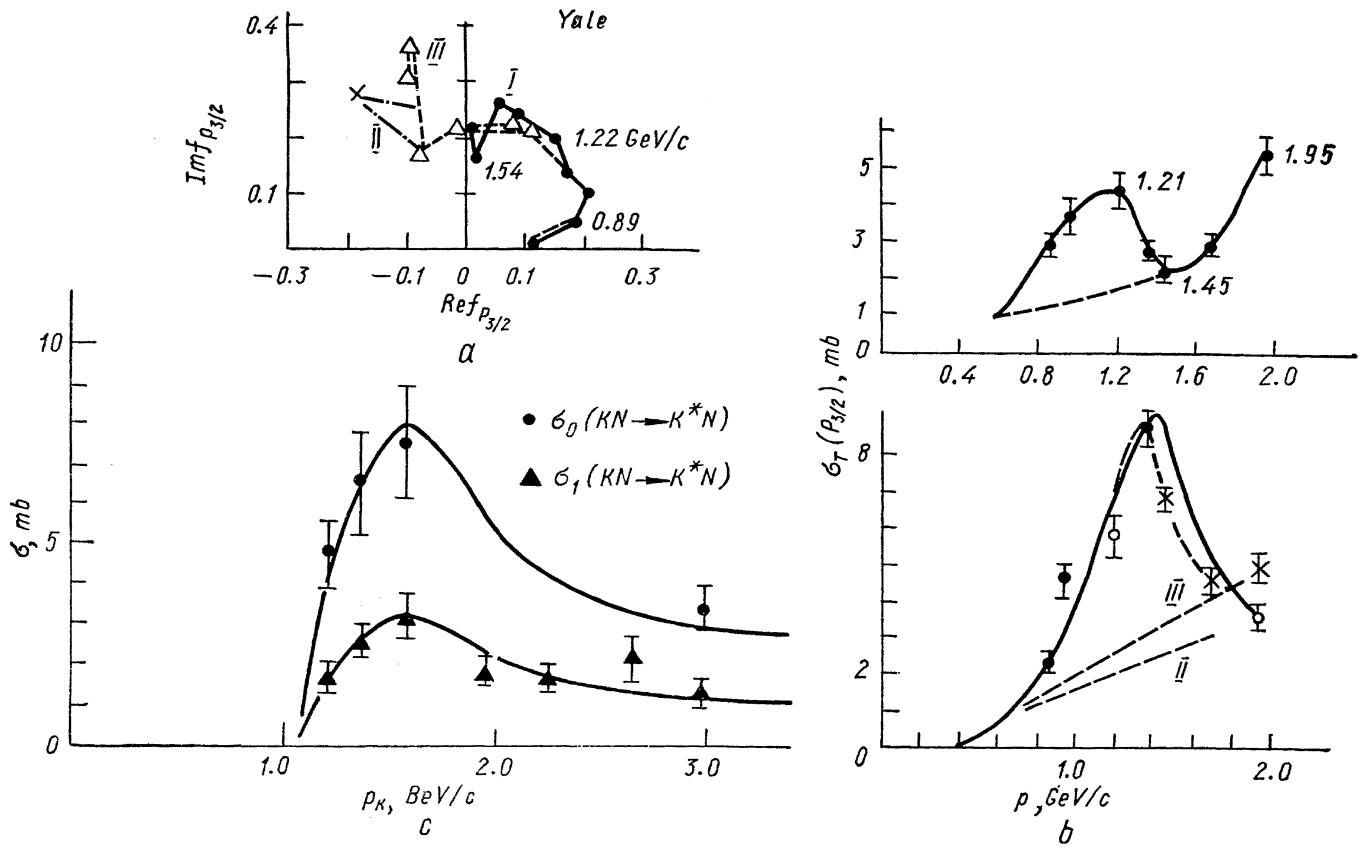

Fig. 3. (*a*) Partial total cross section, $\sigma_T(P_{3/2})$, of the $P_{3/2}$ partial wave for solution I. (*b*) $\sigma_T(P_{3/2})$ for solutions II and III (Argonne, Maryland, Northwestern, NAL). The dotted lines indicate the assumed backgrounds.

change of the P_3 amplitude has also been performed by this last group and is also shown in Fig. 4 where a possible small change occurs at the expected beam momentum. This is to be contrasted with the conclusion of the University College London — Rutherford group which has performed a similar analysis, results shown in Fig. 5, in which four possible solutions (A — D) are displayed. Three of the possibilities have a negative S wave even up to higher energies and of these one has a possible resonant $P_{3/2}$ partial amplitude (in agreement with the other groups) with the $P_{3/2}$ going through the center of the Argand plot, i. e. phase shift completely undetermined. The authors, however, favor solution B, nonresonant $P_{3/2}$ wave, on the basis of the accompanying attractive S wave amplitude for energies > 0.8 *GeV* which agrees with the latest analysis of Donnachie and Carreras [12]. This latter work is a Regge pole model fit to K^+p data and has the feature of fitting the dip in K^+p total cross section and reversing the S wave from repulsive at low energies to attractive at high energies. Therefore a crucial question is the behavior of the S wave amplitude at energies greater than 0.5 *GeV*, if repulsive, a resonant solution for $P_{3/2}$ is favored, if attractive, non-resonant. Returning once again to the question of the speed of the $P_{3/2}$ amplitude, a CERN—Saclay [13] group has also analyzed the pertinent data, the results of which are shown in Fig. 5, in which there is no perceptible change in the speed of the $P_{3/2}$ wave to be contrasted with the clear change in the well-known resonant P_{33} amplitude for the π nucleon case.

The BGRT collaboration has taken a different tack, in that the energy dependence of the phase shifts has been fixed in performing the amplitude analysis. Again, numerous solutions are found among which is the one shown in Fig. 6 where the $P_{3/2}$ amplitude traverses a counterclockwise circle in the Argand plot,

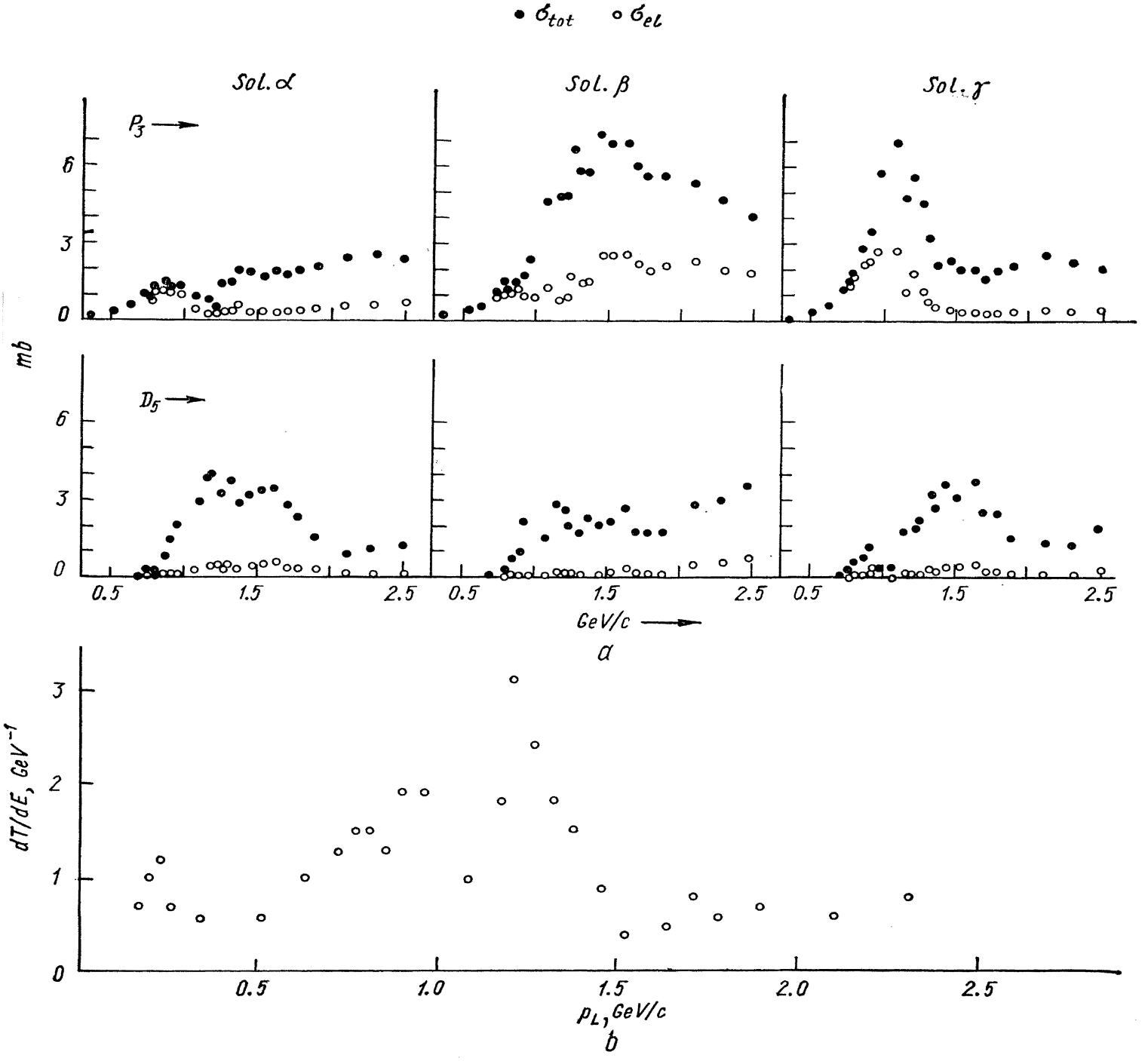

Fig. 4. CERN. K^+p partial wave cross sections (a). (b) Speed of P_3 in K^+p elastic scattering. Solution γ.

again favoring a resonant interpretation. It should be emphasized that all these separate analyses are not independent since all the practitioners of these amplitude analyses use all the same available data. As noted earlier, the experimental data agree very well, and this is further illustrated in the case of the inelastic channels in Fig. 7 where the partial cross sections are displayed. One can summarize the status of the $I = 1$ bump at $M = 1900$ as unresolved, with four groups favoring a resonant interpretation and one group non-resonant.

As noted earlier, there is also evidence for a possible Z^* in the $I = 0$ state in the 1870 MeV mass region. As pointed out by Hirata et al. [14], this increase in cross section is associated with the onset of single pion production, namely K^*N

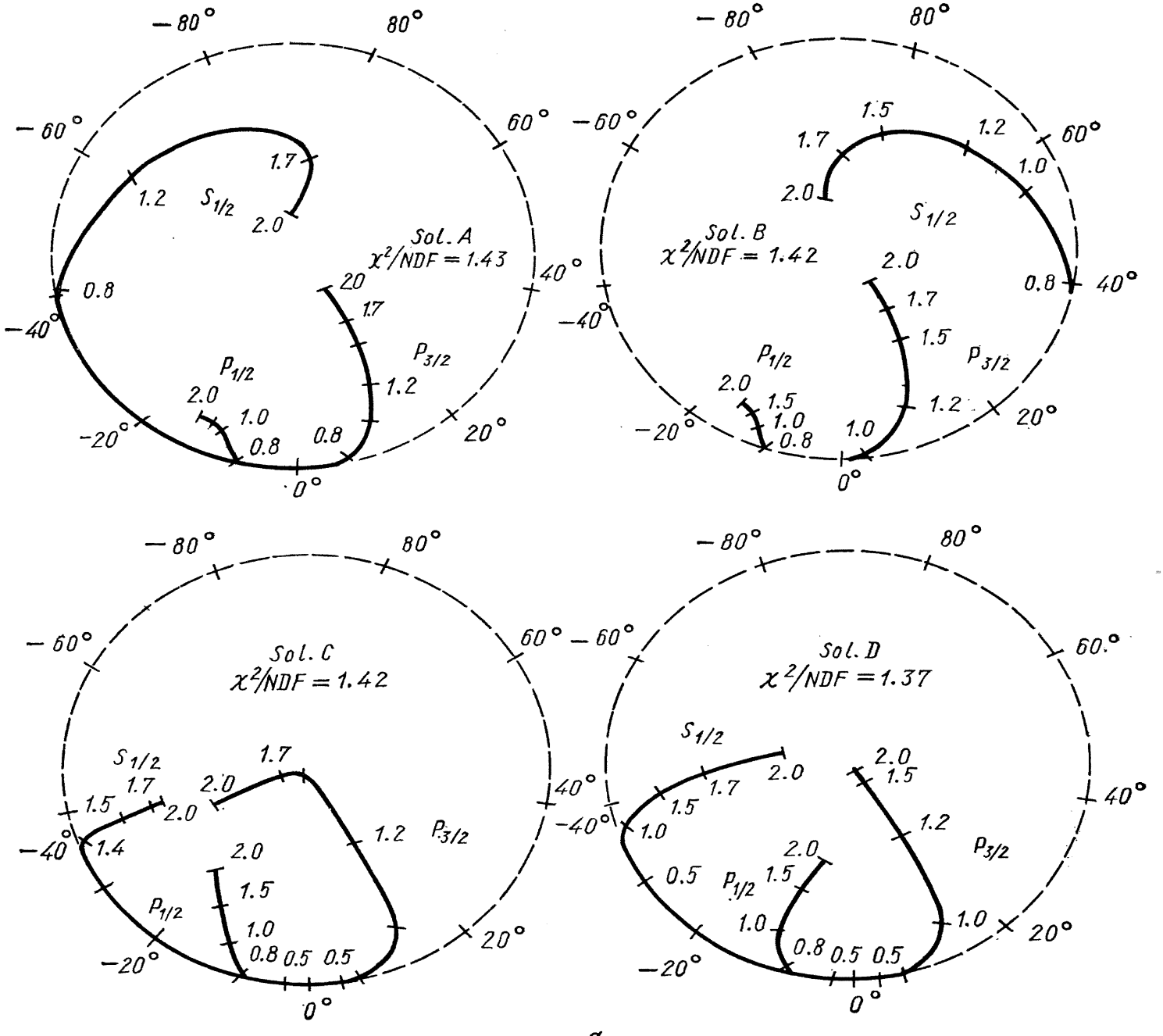

Fig. 5. (*a*) U. C. London + Rutherford Lab. The S- and P-wave amplitudes for the four phase
(*b*) CEN — Saclay. Experimental speeds (in 0.1 GeV^{-1}) for, respectively, P_{13} (solutions I_A and
to speeds for fits with Breit — Wigner term + background

formation as shown in Fig. 3, and this has been verified by the recent work of the BGRT collaboration presented at this Conference. Unfortunately the limited analysis is not very conclusive, the main features being the presence of several partial waves in the channel and the production mechanism being mainly due to π exchange in the t channel to be contrasted with ω, ρ exchange for the $K\Delta$ final state. However, the continued exploration of the K^+p and K^+d total cross section to lower energies has unveiled the presence of another possible Z^*. The main contributors to the study of $I = 0$ Z^* are shown in Table II. Referring to Fig. 1,

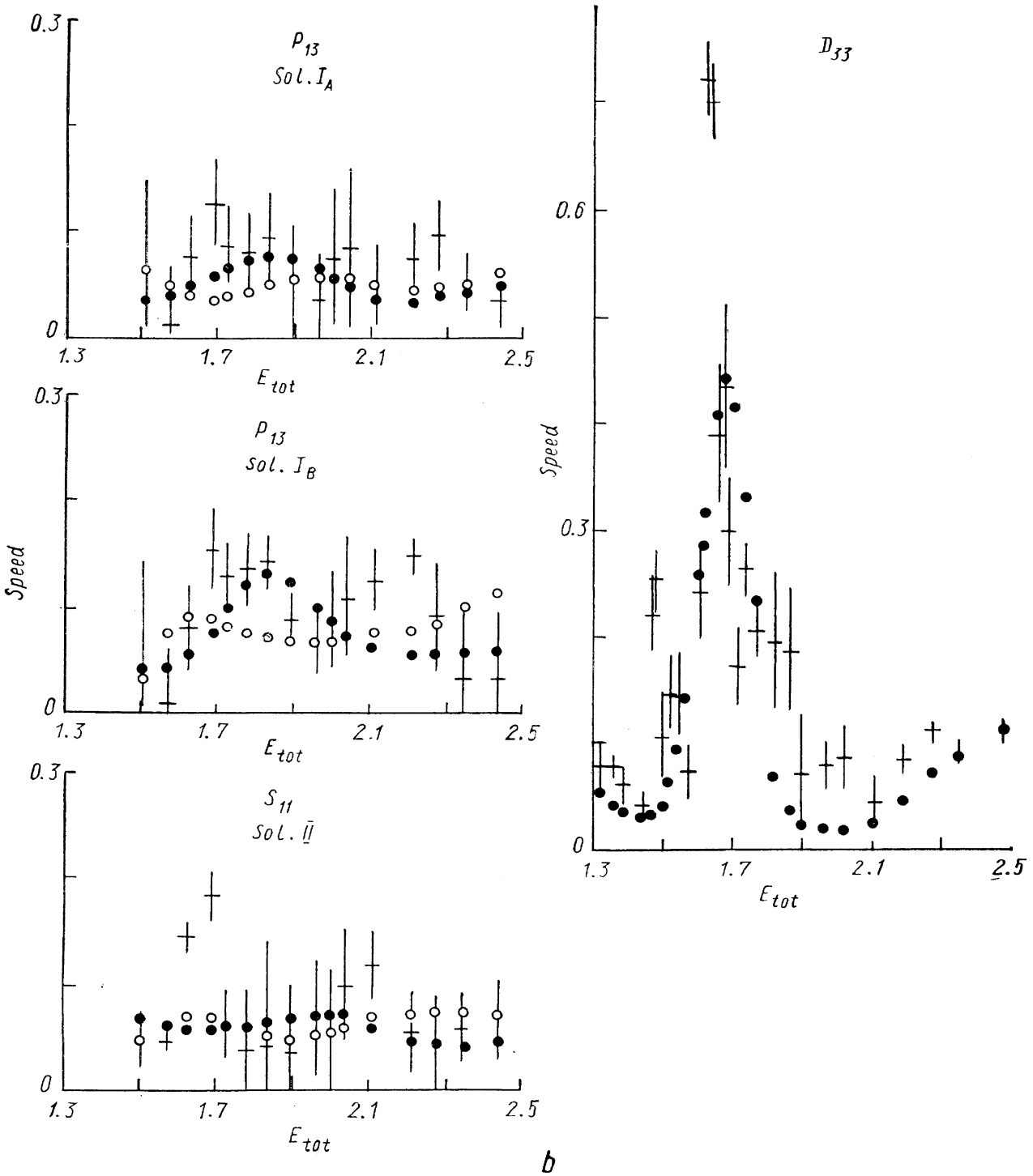

b

shift solutions described in the text. For clarity, they are only shown at a few momenta. I_B), S_{11} (solution II) and D_{33} of pion-nucleon phase-shift analysis. Solid points correspond and open points to speeds for fits with background alone.

Table II

Z_0^*	$I = 0$, $M = 1780$ *MeV*, $\Gamma \approx 500$ *MeV* $M = 1870$ *MeV*, $\Gamma \approx 160$ *MeV* σ_T, $\sigma_{\text{inelastic}}$, $d\sigma/d\Omega$
σ_T	1. BNL (Cool et al.) 2. Rutherford (Bugg) 3. Arizona (Peterson/Jenkins)
$\sigma_{\text{inelastic}}$	1. Berkeley (Hirata) 2. BGRT (Hughes)

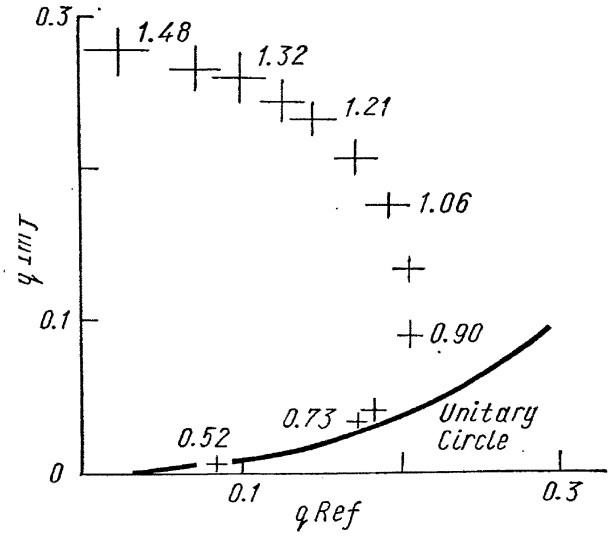

Fig. 6. BGRT. Argand diagram for P_{13} amplitude.

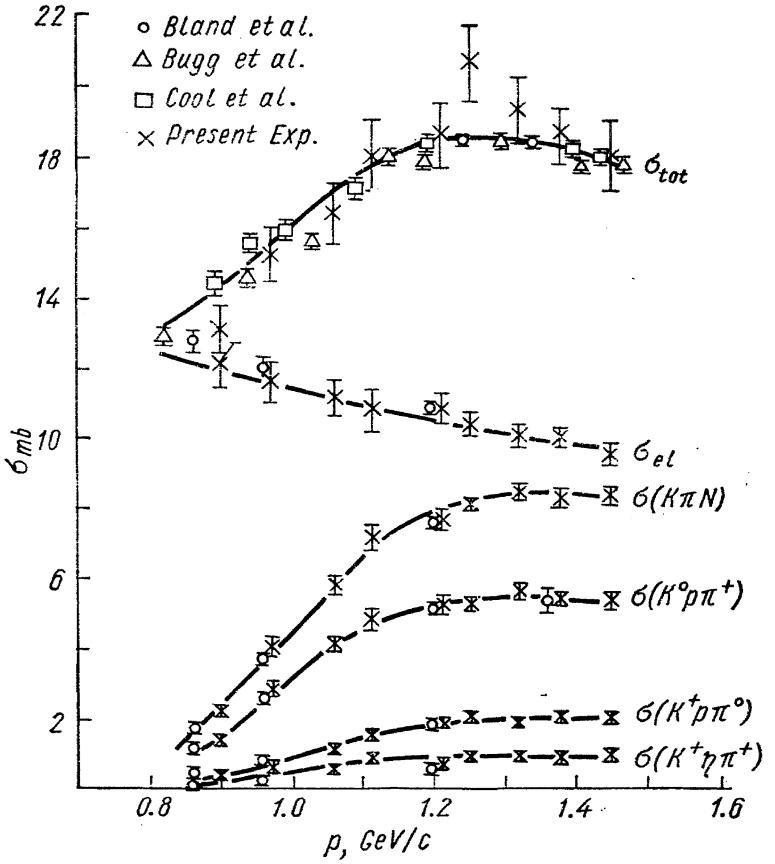

Fig. 7. BGRT collaboration. K^+p cross sections.

one notes the sharp drop in the K^+p cross section at $P_{K^-} \approx 750$ *MeV/c* in contrast to the relatively smoothly varying K^+d cross section in this same momentum region. The experimental data are those of Bugg et al. [15] and Bowen et al. [16]. The K^+p experimental values agree rather well, while there is an 8% discrepancy in the K^+d total cross section values. The unfolding of the $I = 0$ cross section, as performed by Abrams et al. [17], is shown in Fig. 1. If one uses the higher values for the K^+d cross section, then one obtains a second clear bump at a mass of $M = 1780$, while the lower points give a shoulder at a similar mass. Averaging the data also yields a two-bump structure. This result is not sensitive to either the Glauber correction or the nuclear Fermi motion as has been especially explored by Lynch [18]. Due to the disparity of the data, the parameters of the possible lower mass Z^* are not precisely known, the mass being $M = 1780$ *MeV* and width $\Gamma = 500$ *MeV*. It occurs below the threshold for single π production so that it is elastic. It is also clearly associated with the charge exchange reaction, shown in Fig. 8, as presented by BGRT, with the total increase of ≈ 4 *mb* in the total $I = 0$ cross section corres-

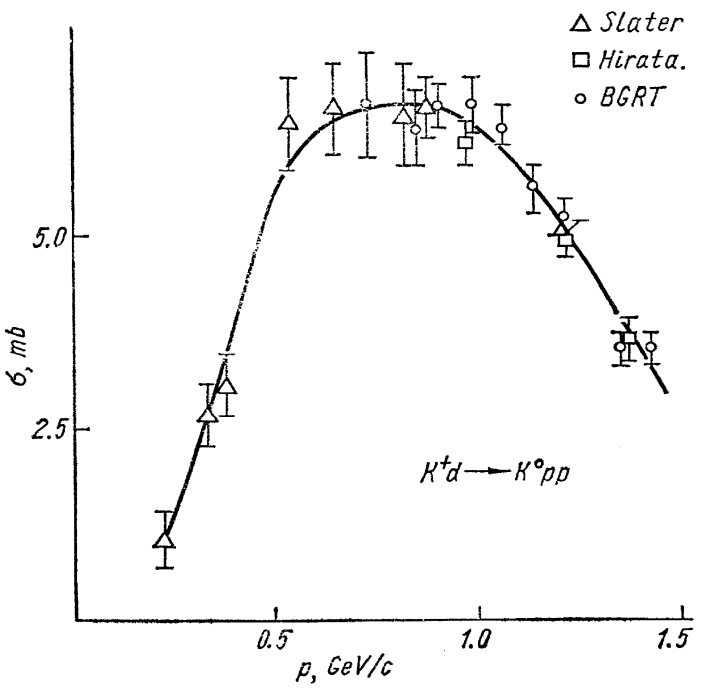

Fig. 8.

ponding to roughly the increase in this latter partial cross section. These data are still to sparse for meaningful partial wave analysis.

The Z^* situation can be summarized by noting that there are now three clear enhancements, two associated with the onset of inelastic channels and one elastic, none of which have been clearly demonstrated to be resonant.

2. Λ, Σ Resonances

This category comprises the most populated of the strange baryons. Such resonances with strangeness $S = -1$ and $I = 0$, 1 have been explored at length by both formation and production experiments. The quantities measured in each type of endeavor are noted in Table III. Although several of

Table III

Formation Experiments

Measure: σ_{total}, σ_i, $d\sigma/d\Omega$

Reactions: $\bar{K}N \to \bar{K}N$ Derive: M, Γ, J^P, I

$\to \Sigma\pi$ $t \approx \sqrt{X_e X_i}$ $X_i = \Gamma_i/\Gamma$

$\to \Lambda\pi$

Production Experiments

Measure: $M^2_{\text{eff}} = E_i^2 - \left|\vec{P}_i\right|^2$, angular correlations

Reactions: $\bar{K}N \to \Lambda\pi\pi$ Derive: M, Γ, X_i, J^P

$\to \Sigma\pi\pi$

$\to K N\pi$

etc.

the pertinent parameters are common to both in many cases, one technique is complementary to the other. For instance, the spin parity, J^P, emerges automatically from the partial wave analysis in formation experiments, while such information is usually poorly known from an examination of the angular correlations (in production experiments). On the other hand, the total and partial widths are reliably derived from the bumps observed in effective mass distributions while such values are more nebulous in formation experiments. As such, the information reported is complementary as well as confirmatory. The inspection of these hyperon resonances can be separated into several classes: 1) those that are clearly seen as a bump in either formation or production experiments, 2) states that are weakly coupled to $\bar{K}N$ system and/or are produced with small cross sections resulting in an uncertainty as to their detailed properties, and 3) very weakly produced states whose existence is in doubt. Examples are displayed in Fig. 9 where the $\bar{K}N$ $I = 0$ and 1 systems exhibit the strongly produced Λ (1815), Λ (2100), and Σ (1765) and the weaker Λ (1690), the Λ (1830) shoulder, Λ (2310), Σ (1915), Σ (2020), and Σ (2250). A similar examination from production experiments of the $\Lambda^0\pi^+\pi^-$ and $\Sigma^0\pi^+\pi^-$ final states is shown in Fig. 10 where the Σ (1660) and Σ (1385) are quite prominent while the Σ (1940) and Σ (2280) are less clearly evident. One also notes the diffusiveness of the $(\Lambda\pi^0)$ effective mass spectrum in the 1600—1800 *MeV* mass region. The main effort over the past few years has been to uncover the properties of these more weakly produced states. The groups that have contributed to the formation experiment endeavors are noted in Table IV, the emphasis at this Conference being at the higher energy region.

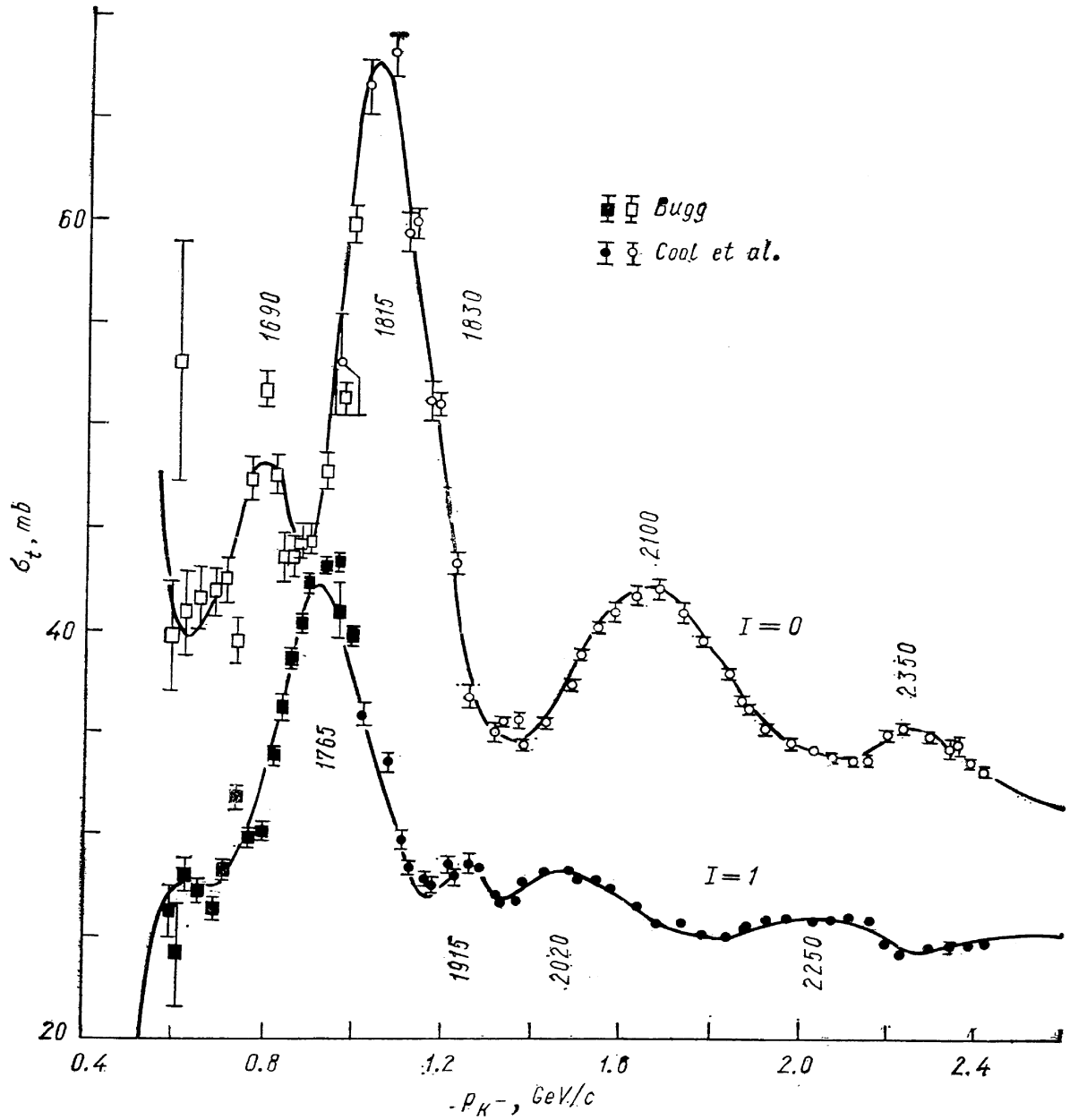

Fig. 9.

Table IV

Formation Experiments

Low Energy	
0—500	1. Berkeley (Tripp/Kadyk)
	2. Columbia (Kim)
	3. Maryland (Sakitt)
	4. BNL — Massachusetts — Yale (Willis)
	5. CHS (Armenteros)
Intermediate Energy	
400—1200	1. CHS
	2. Chicago — Heidelberg (Levi — Setti)
	3. Pisa — BNL — Yale (Berley)
High Energy	
>1100	1. CHS (Pagiola)
	2. Berkeley (Ely)
	3. College de France — Rutherford — Saclay (CRS)
	4. Birmingham — Edin — Glasgow — Imperial College

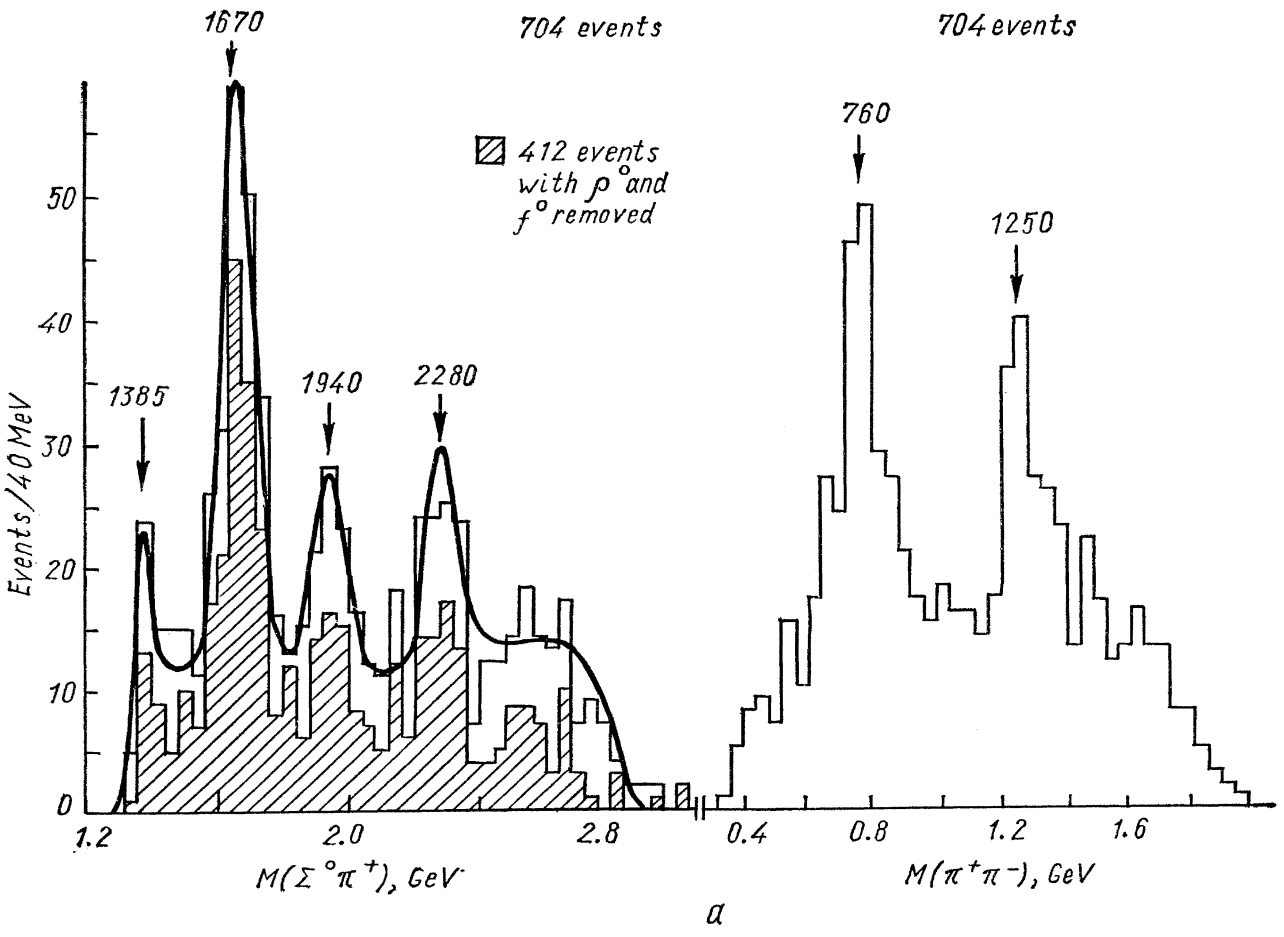

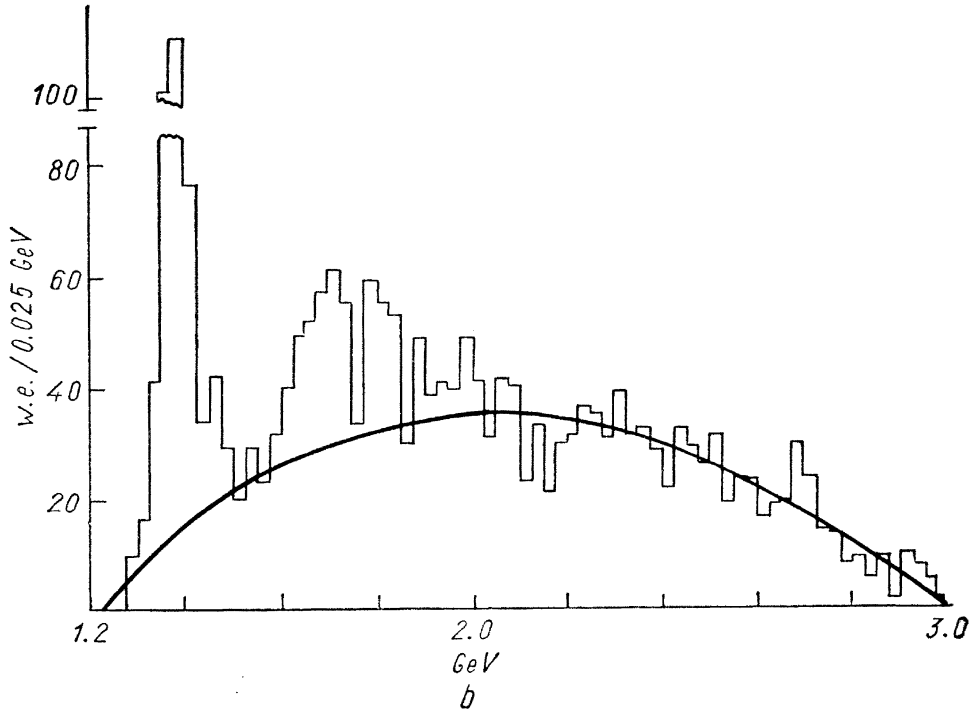

Fig. 10. (*b*) $M(\Lambda\pi^+)$. 2181 entries, 2364 weighted entries (w. e.)

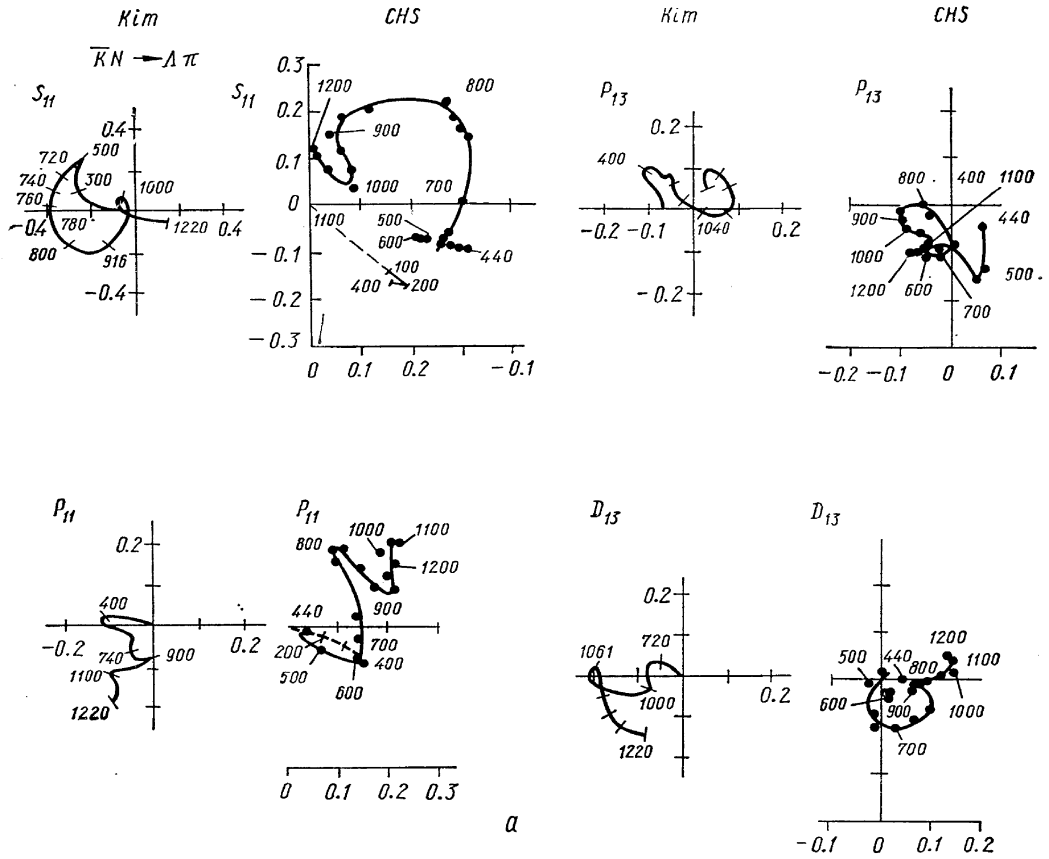
Kim
CHS
Kim
CHS
$\bar{K}N \to \Lambda\pi$
S_{11}
S_{11}
P_{13}
P_{13}
P_{11}
P_{11}
D_{13}
D_{13}
a

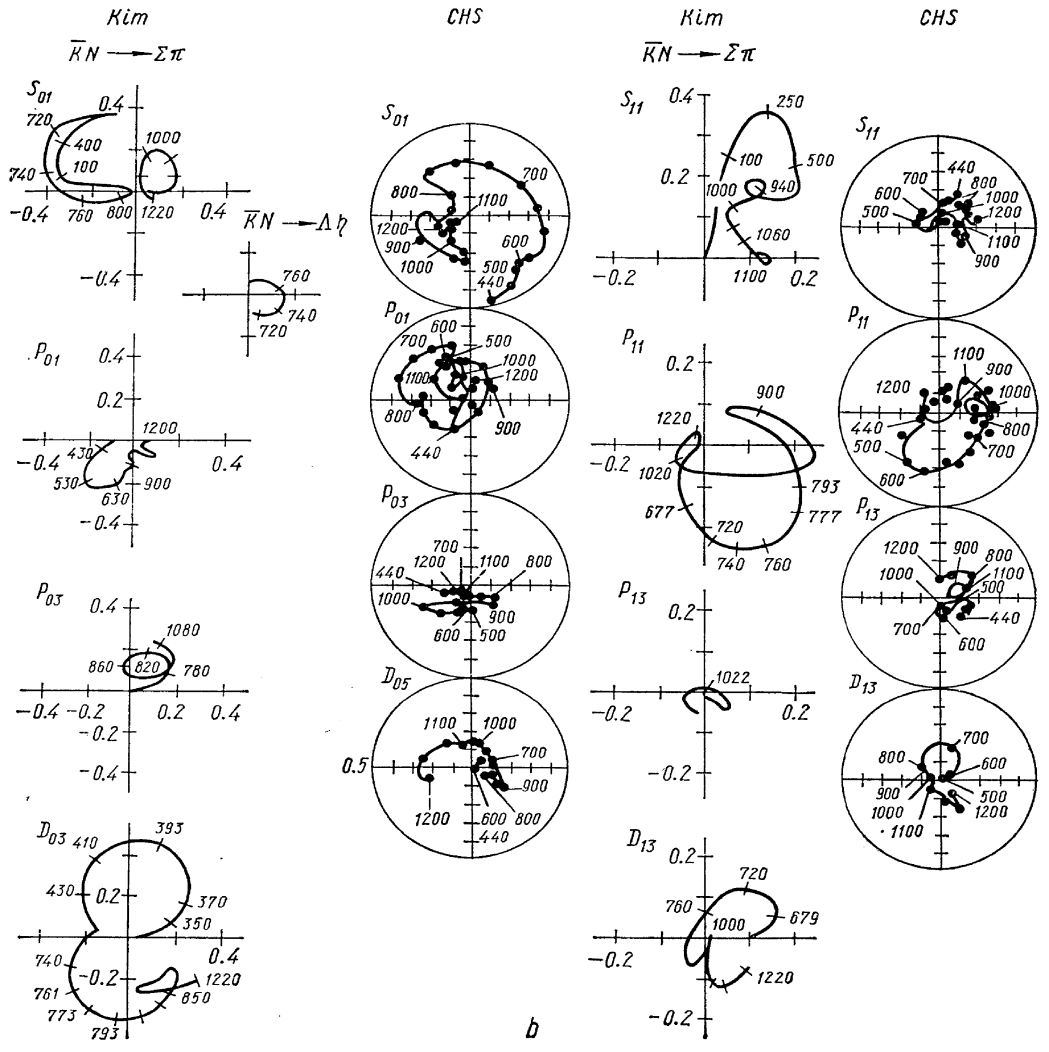
Kim
CHS
Kim
CHS
$\bar{K}N \to \Sigma\pi$
$\bar{K}N \to \Sigma\pi$
$\bar{K}N \to \Lambda\eta$
S_{01}
S_{01}
S_{11}
S_{11}
P_{01}
P_{01}
P_{11}
P_{11}
P_{03}
P_{03}
P_{13}
P_{13}
D_{03}
D_{05}
D_{13}
D_{13}
b

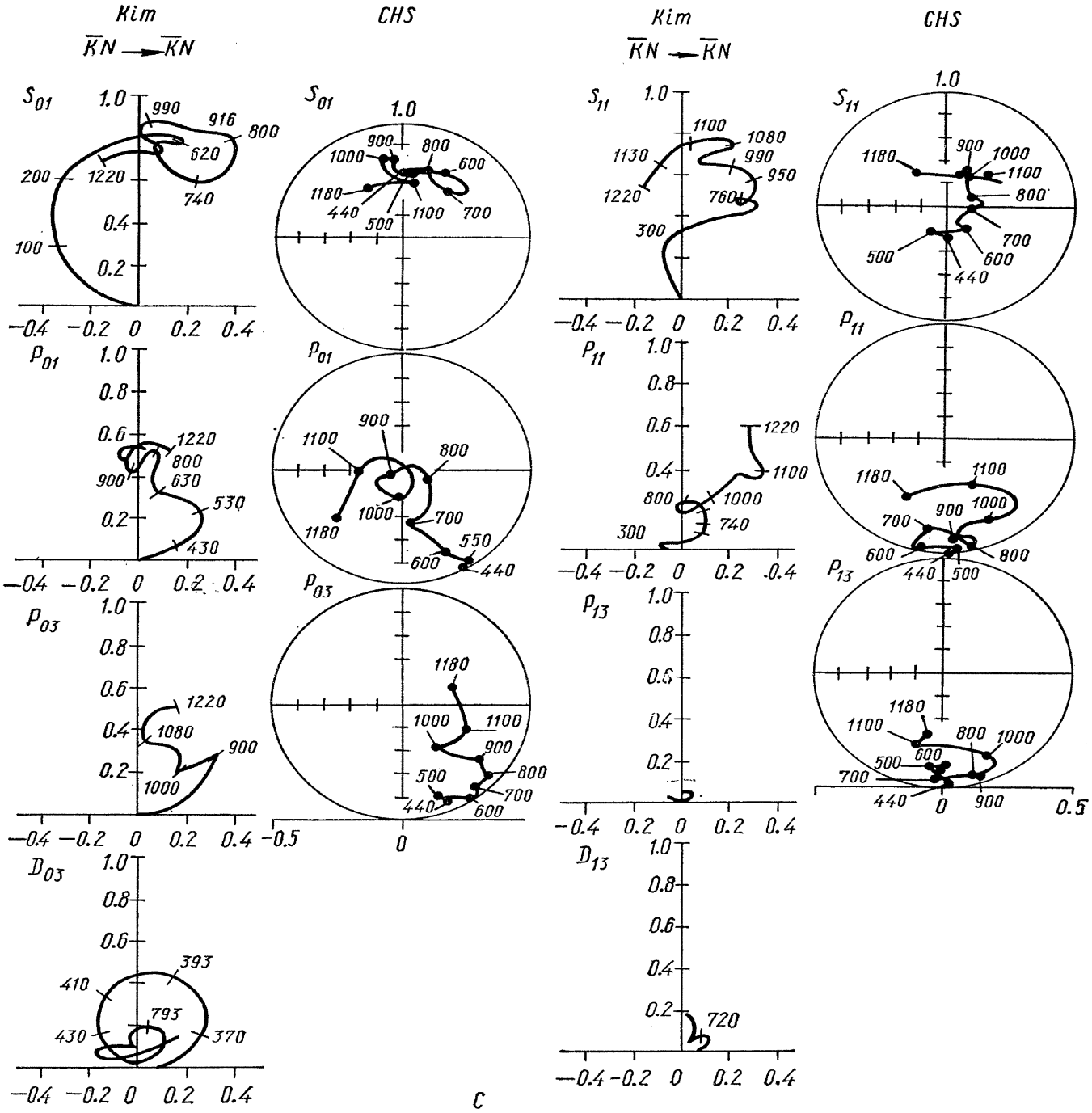

Fig. 11.

The analysis procedures by nearly all the groups is the energy dependent approach. This is illustrated in Table V. The measured differential cross sections and polarizations are parameterized in terms of Legendre (P_l) and associated Legendre (P_l^1) polynomials. The resultant coefficients a_l, b_l are then re-expressed in terms of the partial wave amplitude A_l. The energy dependence of each amplitude is then expressed as a background and resonance term. The form of the resonance amplitude is a standard Breit Wigner and that of the background is a polynominal (or exponential) in terms of the incoming particle momentum, k. A variation on the energy independent method (described in the Z^* section) has been adopted by the CERN — Heidelberg — Saclay collaboration, the so-called partial independent method. In this case, all possible solutions are found at each particular energy; however, this procedure is begun at the very low energies where

only a few partial waves exist. These solutions then serve as starting values for the next higher energy and so on. In this manner, the multiplicity of possible solutions is severely reduced to a few per energy. This method is best applied to the $\Lambda\pi$ system which is pure $I = 1$ state and where polarization information is readily available via the Λ decay, then to the $\Sigma\pi$ channel which is an isospin 0 and

Table V

Energy Dependent

$$\frac{d\sigma}{d\Omega} = \sum_l a_l P_l (\cos\theta) \quad \frac{P d\sigma}{d\Omega} = \sum_l b_l P'_l (\cos\theta)$$

$$A = A_{\text{background}} + A_{\text{resonance}}$$

$$A_{\text{bdg}} = (c + dk + ek^2) + i(f + gk + hk^2)$$

$$A_{\text{res}} = \frac{\sqrt{X_e X_i}}{[2(E_R - E)/\Gamma] - i}$$

1 mixture in addition to having poorer polarization information, and last to the $\bar{K}N$ system where very little polarization information is available.

A third approach has recently been applied at these higher energies by Kim [19]. This involves the K matrix and effective range formalism as originally proposed by Dalitz and Tuan [20] and extended by Ross and Shaw [21]. It is a multichannel procedure, the $\Lambda\pi$, $\Sigma\pi$, and $\bar{K}N$ final state distributions being fit simultaneously. The elements of the symmetric K matrix which are real and the r matrix are related to the partial wave amplitudes. Such an analysis has been quite standard in the low energy region 0—500 *MeV/c*. The innovation has been to make the r matrix nondiagonal, to allow for inelastic channels, and to extend

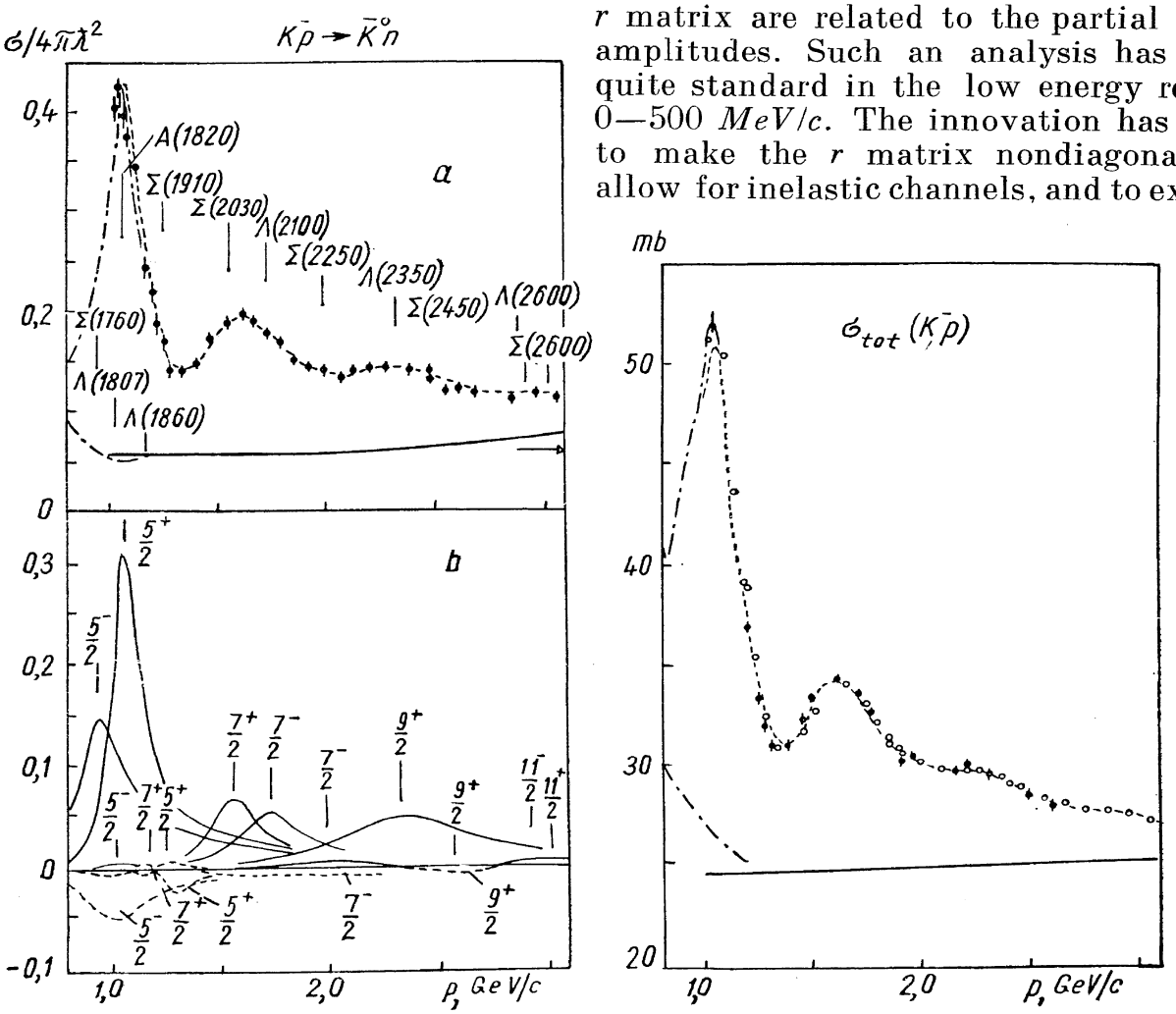

Fig. 12.

the analysis up to 1200 *MeV/c*. This latter feature is performed in 100 *MeV/c* steps keeping the *K*-matrix components fixed but allowing the elements of the *r* matrix to vary. Allowing *S*, *P*, and *D* waves gives 64 parameters for the *K* matrix and 64 parameters in the *r* matrix to be determined.

A comparison of the results from both the CHS (partial independent) and Kim *r* matrix approach is shown in Fig. 11. The complex S, *P*, *D* wave amplitudes are plotted on Argand diagrams for each of the three reactions $\bar{K}N \to \Lambda\pi$, $\Sigma\pi$, and $\bar{K}N$. The S_{01} Λ (1670), $D_{03}\Lambda$ (1520), Λ (1690), and $D_{13}\Sigma$ (1660) resonances are clearly evident. The unresolved questions are the existence of the other possible resonances, smaller circles, wiggles, etc. on the Argand plots. One notes the difficulty of assessing the validity of the various claims from an examination of such figures. A further illustration of the formation experiment approach is shown in Fig. 12 in which the charge exchange ($K^-p \to \bar{K}^0n$) reaction was studied in conjunction

Table Va

Resonances	J^P	Mass (*MeV*)	Width (*MeV*)	Elasticity
Σ (1760)	$5/2^-$	[1768]	[128]	[0.45]
Λ (1807)	$5/2^-$	[1807]	[123]	[0.09]
Λ (1820)	$5/2^+$	1825±1	80±6	0.65±0.02
Λ (1860)	$7/2^+$	1877±6	24±15	0.07±0.02
Σ (1910)	$5/2^+$	1906±6	50±12	0.07±0.02
Σ (2030)	$7/2^+$	2049±4	126±11	0.27±0.02
Λ (2100)	$7/2^-$	2121±5	147±15	0.24±0.02
Σ (2250)	$7/2^-$	2237±11	164±50	0.04±0.03
Λ (2350)	$9/2^+$	2358±6	324±30	0.22±0.05
Σ (2450)	$9/2^+$	[2455]	[140]	0.01±0.01
Λ (2600)	$11/2^-$	[2585]	[300]	0.02±0.02
Σ (2600)	$11/2^+$	[2620]	[175]	0.06±0.02
Backgrounds		*a*	*b*	*c*
$\sigma_{\bar{K}^0n}/4\pi\lambda^2$		0.072±0.002	−0.020±0.001	0.007±0.001
σ_{tot} (*mb*)		24.53±0.96	0.06±0.97	0.04±0.23

with the K^-p total cross section. The amplitude analysis by Bricman et al. [22] yields the spin-parity assignment as well as elasticities for many states in the 1800—2600 *MeV* mass region as noted in the Table Va.

A summary of pertinent numbers concerning numerous intermediate mass resonances are enumerated in Table VI. Since most experiments quote the amplitude $t \approx \sqrt{X_e X_i}$ while Kim quotes the branching fraction X_i; in the former case I have calculated the X_i from the t_i in order to perform a comparison. The agreement is quite good for the Λ (1670), Λ (1690), and Σ (1665). For the higher mass states the main measured quantity is the elasticity, yielding $t_{\bar{K}N}$, where again there seems to be a consensus. A great deal of effort has recently been expended on investigating the Σ (1915) and Σ (2030) resonances. In particular, the work of CRS [23] and Ely et al. [24] on the $\Sigma\pi$ and $\Lambda\pi$ final states has verified the spin-parity assignment of $5/2^+$ and $7/2^+$ respectively, obtained consistent values for $t_{\Sigma\pi}$ and $t_{\Lambda\pi}$, and measured the relative phases of these amplitudes with respect to each other and other well-established resonances. The coupling of the Σ (1915) to $\bar{K}N$ is quite weak, the best measurement being 0.07 ± 0.02 so that the $\Sigma\pi$ and $\Lambda\pi$ branching fractions are poorly determined. On the other hand,

Table VI

		$t_{\bar{K}N}$	$t_{\Sigma\pi}$	$t_{\Lambda\pi}$ $t_{\Lambda\eta}$	$X_{\bar{K}N}$	$X_{\Sigma\pi}$	$X_{\Lambda\pi}$	$X_{\Lambda\eta}$	X_{other}
Λ (1670) $1/2^-$	CHS	.17∓.05	—.28∓.05	+.26	.17	.45		.39	
	Berkeley		—.29∓.03						
	Kim				.30	.59		.11	
Λ (1690) $3/2^-$	CHS	.18∓.05	—.36∓.05	0∓.05	.18	.72			
	Berkeley		—.31∓.05						
	Kim				.20	.75			
Σ (1665) $3/2^-$	CHS	.08∓.05	.20∓.05	.10+.05	.08	.50	.125		
	Kim				.08	.36	.06		.50
Λ (1830) $5/2^-$	CHS	.09∓.05	—.15∓.05						
	CHH	.08							
	Berkeley (Ely)		—.13						
Σ (1915) $5/2^+$	Cool	.10							
	Daum	.12							
	CHS/CRS	.07∓.05	—.08∓.05	—.09∓.05	.10	.10	.10		
	Berkeley (Ely)		—.14∓.05	—.085∓.01					
Σ (1940)	CRS	$A\Sigma$ (1915) = $= A\Sigma$ (1760) — $\Lambda\pi$ $A\Sigma$ (1915) = $= -A\Sigma$ (2030) — $\Lambda\pi$ $A\Sigma$ (1915) = $= A\Sigma$ (2030) — $\Sigma\pi$ $A\Sigma$ (1915) = $= A\Sigma$ (1815) — $\Sigma\pi$							
	Bubble Chamber				.17∓.24	.64∓.31	.19∓.19		
Σ (2030) $7/2^+$	CHS	.27+.05							
	CRS	.19+.03	—.09∓.02	.20∓.02					
	Glasgow/ Imperial College	.17+.04							
	Cool	.10							
	Daum	.11							
	Wohl	.27							
Λ (2100) $7/2^-$	Cool	.33							
	Daum	.33							
	Wohl	.25							
	CHS	.24∓.05							
	CRS	.35∓.04 (width too large)							
		.19∓.03	.16∓.02						

Contin. table VI

		$t_{\bar{K}N}$	$t_{\Sigma\pi}$	$t_{\Lambda\pi}$ $t_{\Lambda\eta}$	$X_{\bar{N}K}$	$X_{\Sigma\pi}$	$X_{\Lambda\pi}$	$X_{\Lambda\eta}$	X_{other}
Σ (2280) $7/2^-$ $9/2^-$	Cool Daum Bricman Bubble Chamber	.08 .04 .04			$.05 \mp .15$	$.77 \mp .23$	$.18 \mp .15$		
Λ (2350) $9/2^+$ $7/2^-$	Kycia Bugg Bricman	.68 .57 .10							
Σ (2450) $9/2^+$	Abrams Bugg Bricman	.26 .30 .10							
Σ (2600) $11/2^+$	Abrams Bricman	.26 .36							

a recent bubble chamber experiment [24] has yielded evidence for a Σ (1940) of unknown spin parity, also with small $\bar{K}N$ branching fraction, but mainly decaying into $\Sigma\pi$ final state. Since the masses and widths agree within their quoted errors, the simplest assumption is that they are the same object. I have therefore used the production results for the branching fraction estimates. For the higher mass states, the main measurements have been with respect to the elastic channels yielding $t_{\bar{K}N}$ and spin parities, all duly noted in this same Table. Needless to say there are numerous other resonances reported by several groups, all supposedly arising from unique partial wave amplitude solutions, however, disagreeing with each other although occurring in the same mass regions. Such possible new resonances are listed in Table VII. There are several Λ, Σ candidates with low values

Table VII

Proposed Resonances

Kim	CHS
Λ (1575) $1/2^+$	Σ (1500—1600) $1/2^+$
Σ (1680) $1/2^-$	Σ (1730) $1/2^-$
Λ (1710) $3/2^+$	Λ (1750) $1/2^+$
Σ (1790) $1/2^-$	Λ (1850) $1/2^+$
Σ (1820) $3/2^+$	
Λ (1790) $1/2^-$	

Other

Σ (1480)	Pennsylvania
Σ (1690)	ANL/Birmingham
Σ (1620)	Brookhaven National Laboratory
Λ (1870) $3/2^+$	CHS (Bricman)
Σ (1900) $1/2^+$	Galtieri/Litchfield (CRS)
Σ (1940) $3/2^-$	Galtieri/Litchfield (CRS)
Σ (2040) $3/2^-$	Galtieri
Λ (2050) $7/2^-$	CRS
Σ (2070) $3/2^+$	Litchfield/BEGI
Σ (2070) $5/2^+$	CRS
Σ (2120) $7/2^-$	Galtieri
Λ (2110) $5/2^+$	CRS

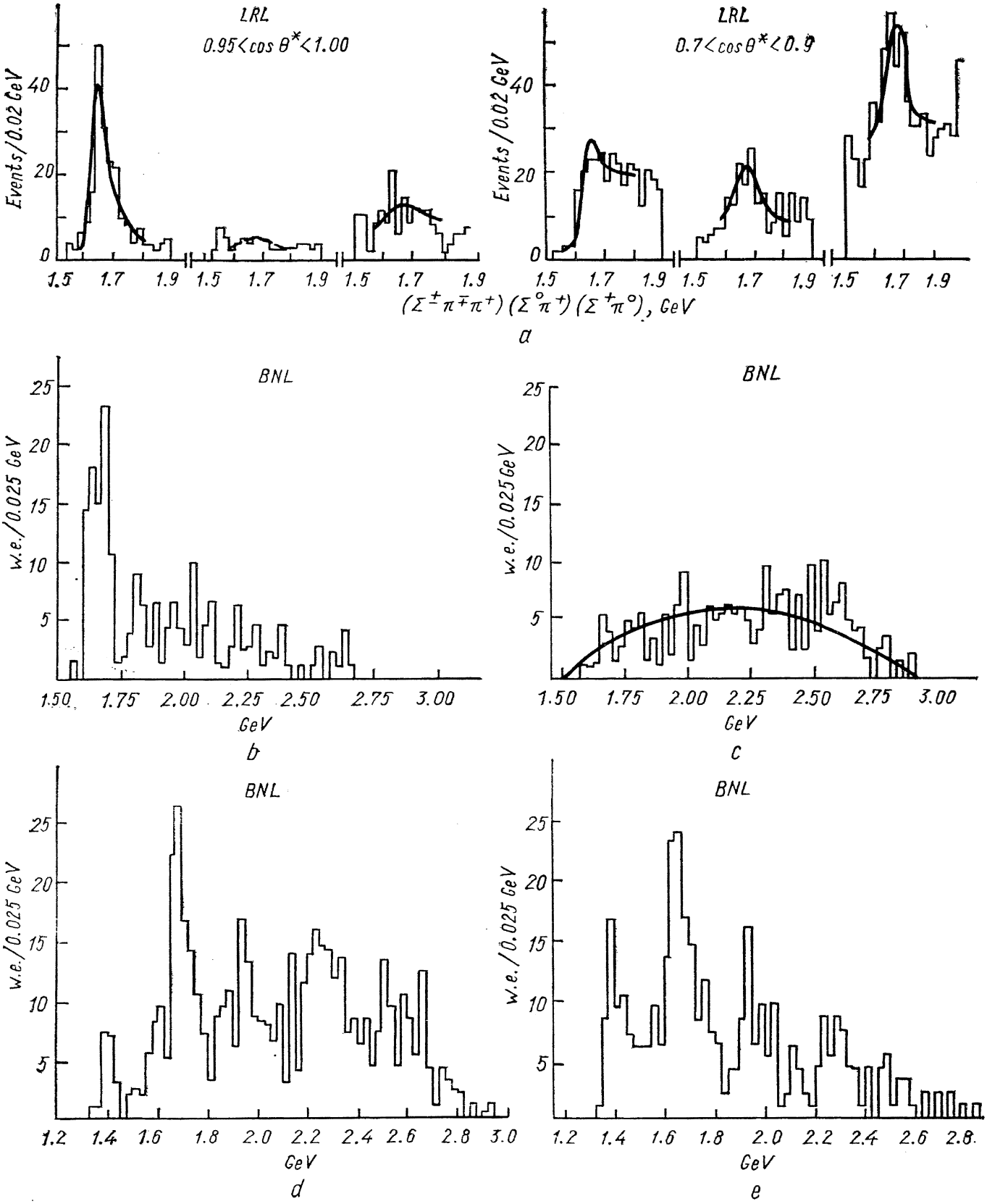

Fig. 13. (*b*) M (Λ (1405) π^+). cos $\theta^* < -0.7$, 108 entries, 204 weighted entries (w. e.). $\lfloor\!\rightarrow \Sigma^+\pi^-$

(*c*) M (Λ (1405) π^+). cos $\theta^* > -0.7$. 159 entries, 224 weighted entries (w. e.). (*d*) M ($\Sigma^0\pi^+$). $\lfloor\!\rightarrow \Sigma^+\pi^-$

cos $\theta^* > -0.7$. 466 events, 502 weighted events (w. e.). (*e*) M ($\Sigma^0\pi^+$). cos $\theta^* < -0.7$. 347 events, 371 weighted events (w. e.).

of spin, $1/2^{\pm}$, $3/2^{\pm}$ as well as a cluster of assorted Λ, Σ states in the 2000 *MeV* region. This list certainly will stimulate extended experimental activity over the next few years.

With respect to production experiments, the main topic I wish to discuss is the question of the Σ (1660). Good evidence for two hyperon states with the same mass, one decaying into $\Sigma\pi$ and the other $\Sigma\pi\pi$ was first reported by Eberhard et al. [26] at Vienna. This observation has since been confirmed by Aguilar — Benitez et al. [27]; the results of both investigations are shown in Fig. 13. The angular distribution of the Σ (1660) $\rightarrow \Sigma\pi$ is certainly less peripheral than that of Σ (1600) $\rightarrow \Sigma\pi\pi$ where the latter consists mainly of Λ (1405) π. A study of the $\Sigma\pi$ mode in formation experiments yields a value of $3/2^-$ for its spin parity. The same value, $3/2^-$, is derived from a study of the $\Sigma\pi\pi$ decay correlations, assuming no interference, in production experiments. The simplest interpretation of the data is the existence of two states with the same mass and same spin parity. As such this interpretation also helps in clarifying the peculiarities of the Σ (1660) decay branching ratios previously observed in production experiments. Referring once more to Fig. 10, one notices the difficulty of determining the Σ (1660) $\rightarrow$ $\rightarrow \Lambda\pi$ branching ratio a problem which is common to most production experiments. The Σ (1690) is intimately connected with the Σ (1660) since its possible existence is completely based on its large $\Lambda\pi/\Sigma\pi$ [28] branching fraction and not on its mass difference which is more difficult to establish. It is quite certain that at incoming K^- momenta less than 5 *GeV/c*, the $\Lambda\pi/\Sigma\pi < 1$ for the Σ (1660) while two experiments at higher momenta report the reverse. There is no additional information concerning the Σ (1690) nor on the controversial Σ (1620) which has been reported to be observed in the $\Lambda\pi$ state produced by K^- interaction at 3.9 *GeV/c* [29] and not observed at 3.0 *GeV/c* [30].

An interesting contribution was presented to this Conferense concerning the possible existence of $S = -1$, but nucleon number $N = 2$, states [31]. The experiment involved neutron interactions in a propane bubble clamber. An examination of the (Λp) effective mass spectrum summing over a variety of final states, see Fig. 14, gives evidence for several possible peaks. These occur at masses of 2058 *MeV*, 2127 *MeV*, and 2252 *MeV*. Again their significance is difficult to evaluate; however, a sum of simple phase space distribution does not seem to explain the data.

In summary of the Λ, Σ resonances, one can say that there are numerous states with well-established properties, some peculiarities such as in the Σ (1660) mass region, and the possibility of many additional resonances.

3. Ξ States

S $= -2$. Although the importance of finding Ξ states was early recognized by experimentalists since all 8 and 10 representations contain such a member, their uncovery was a more difficult matter. This is due to 1) such states can only be studied via production experiments (formation experiments not being possible as a result of the absence of $S = -2$ bosons) and 2) small cross sections. This latter point is illustrated in Fig. 15 where the cross section for two-body production of the Ξ (1320) and Ξ (1530) is plotted as a function of lab momentum. They both decrease as p^{-4} with a high point of $\approx$ 100 μb and reaching $\approx$ $\approx$ 2—5 μb at energies of $\approx$ 4—5 *GeV/c*. The actual peak of the cross section depends on many factors, availability of S channel resonances, etc. but for some limited number of cases, it occurs $\approx$ 200—300 *MeV* above threshold. As a result, the momentum

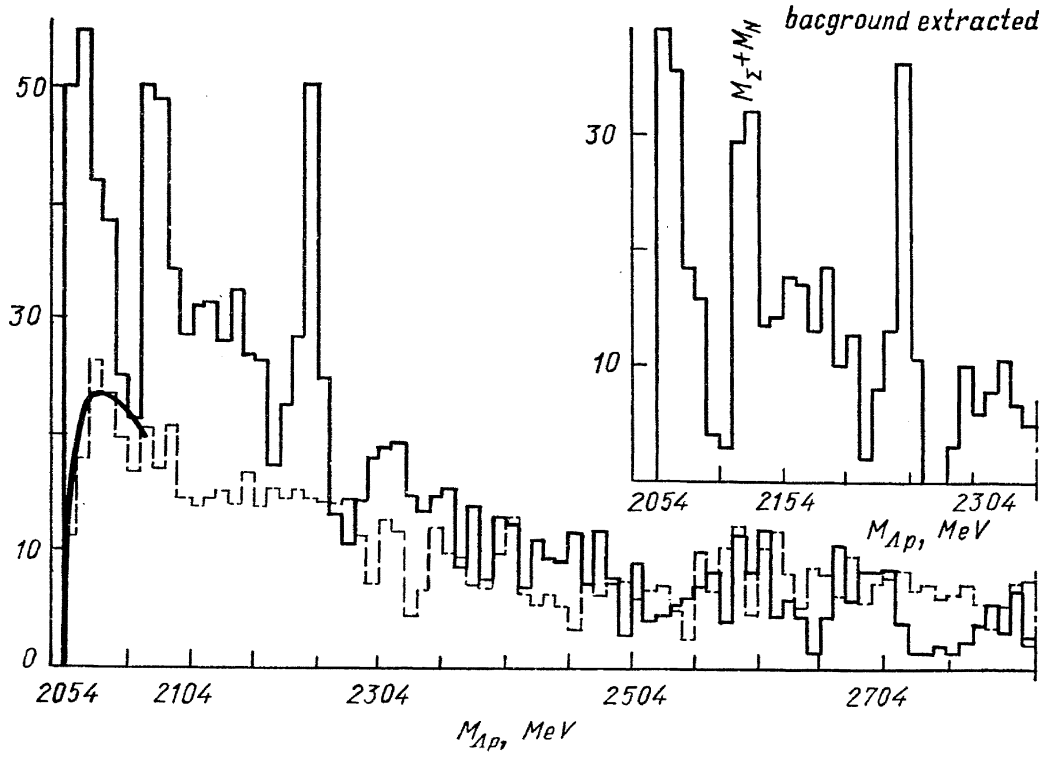

Fig. 14. $nC_6^{12} \to p\Lambda$; $N = 798$ including 205 proton — like interactions $B = 2$, $Q = 1$, $S = 0$

$$nC_6^{12} \to p\Lambda \times$$
$$\times (K^0 m\pi^0) \begin{pmatrix} A_1 \\ Z_1 \end{pmatrix}$$
$$\to p\pi^+\pi^- \times$$
$$\times (K^0 m\pi^0) \begin{pmatrix} A_2 \\ Z_2 \end{pmatrix}$$
$$\to p2\pi^+2\pi^- \times$$
$$\times (K^0 m\pi^0) \begin{pmatrix} A_3 \\ Z_3 \end{pmatrix}.$$

Smooth and dotted lines — impulse approximation normalized to total weight $\Sigma g_i = 1233.7$.

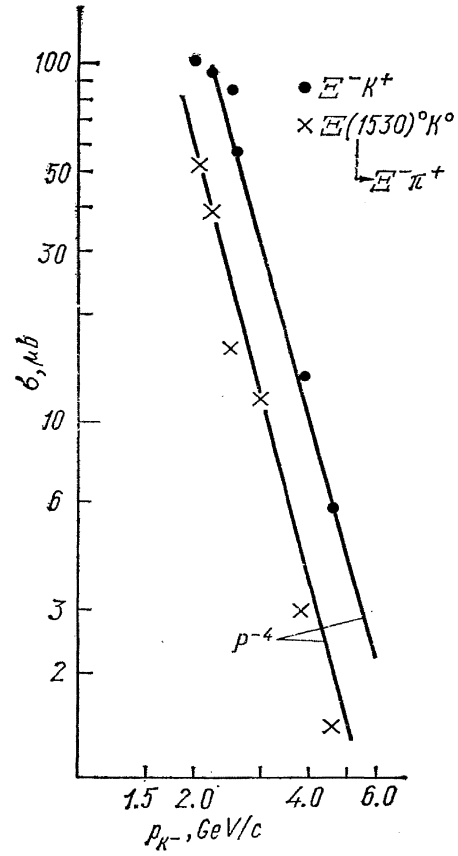

Fig. 15.

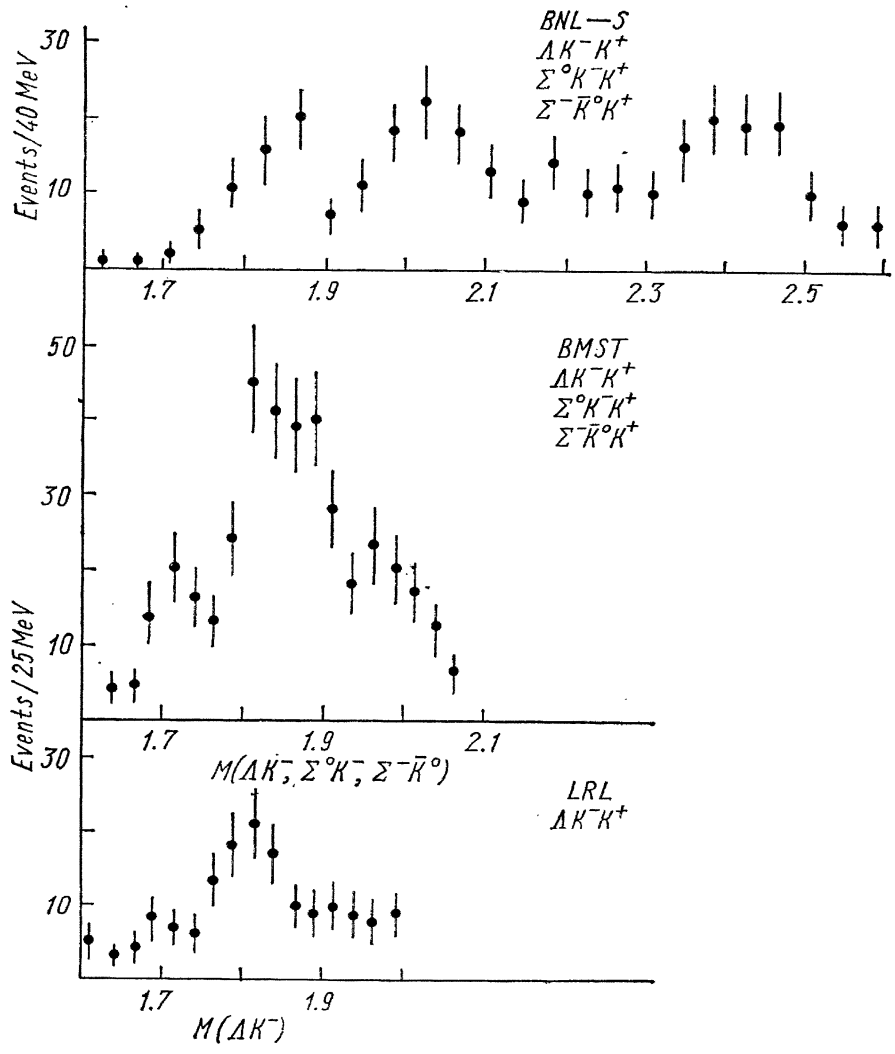

Fig. 16.

band over which a particular resonance is produced with a reasonable cross section is rather limited. In spite of these difficulties some progress has been made, and this is summarized in the succeeding figures. The published Ξ states, in addition to the Ξ (1320) and Ξ (1520), are the Ξ (1820), Ξ (1930), Ξ (2030), Ξ (2430) seen in more than one experiment and the Ξ (1640), Ξ (2240). In Fig. 16 the (ΛK^-) and (ΣK^-) effective mass spectra are analyzed for the LRL (2.7 *GeV/c*) [32], BMST (2.9 *GeV/c*) [33], and BNL (4.6 *GeV/c*) [34] experiments. The Ξ (1820) is clearly evident in all these plots, the quoted masses and widths varying somewhat, however, in agreement with each other within the limited statistics available. Two additional states are observed in the highest energy data, the Ξ (2030) and Ξ (2430), each of 3σ significance.

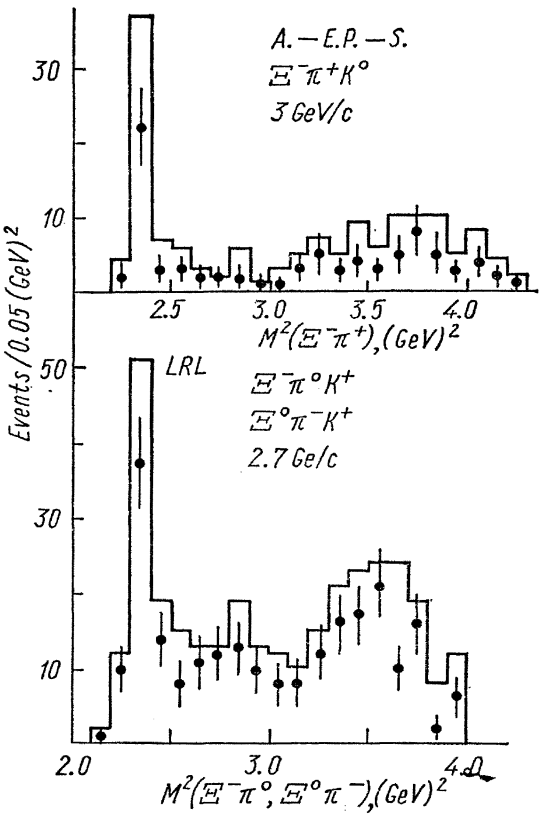

Fig. 17.

The Ξπ modes are less clear, possibly due to the existence of several closely spaced resonances. The original evidence for the anomaly in the 1800 — 1900 mass region is shown in Fig. 17. The histogram contains all the events while the points with associated errors have the *K* (890) events removed. Both the Amsterdam — Ecole Polytechnic — Saclay collaboration [35] and LRL [36] experiments showed deviations from phase space at the higher end of the (Ξπ) effective mass plots, however, in different charge states, Amsterdam (neutral), LRL (negative). The vertical lines indicate the Ξ (1820) and Ξ (1930) regions. Subsequently the BNL — Syracuse collaboration observed a clear Ξ (1930) signal in a channel

Table VIII

Ξ States	
Well Established	
Ξ (1320) 1/2	
Ξ (1530) $3/2^+$	
Ξ (1820)	$\Lambda\overline{K}$, $\Sigma\overline{K}$, Ξπ
Ξ (1930)	Ξπ, Ξππ
Reasonable	
Ξ (2030)	$\Lambda\overline{K}$, $\Sigma\overline{K}$, $\Lambda\overline{K}\pi$
Ξ (2430)	$\Lambda\overline{K}$, $\Sigma\overline{K}$, $Y\overline{K}\pi$
Possible	
Ξ (1635)	Ξπ
Ξ (1762)	Ξπ
Ξ (2240)	$Y\overline{K}\pi$, Ξππ

free from *K* (890) interference effects. This is displayed in Fig. 18. Recently the BMST collaboration, at 2.9 *GeV/c*, has presented evidence for the existence of two (Ξπ) states at masses $\approx$ 1800 *MeV* and 1950 *MeV*. The relevant data are displayed in Fig. 18 where the histogram encompasses all the events while the points with errors refer to events in which the *K* (890) has been eliminated. Excluding the region of the Ξ (1530) a fit to the histogram with one resonance plus background yields a χ^2 of 48 for 24 bins (rather poor) while inclusion of a second resonance reduces the χ^2 to 26 for the same number of bins which is quite acceptable. This splitting

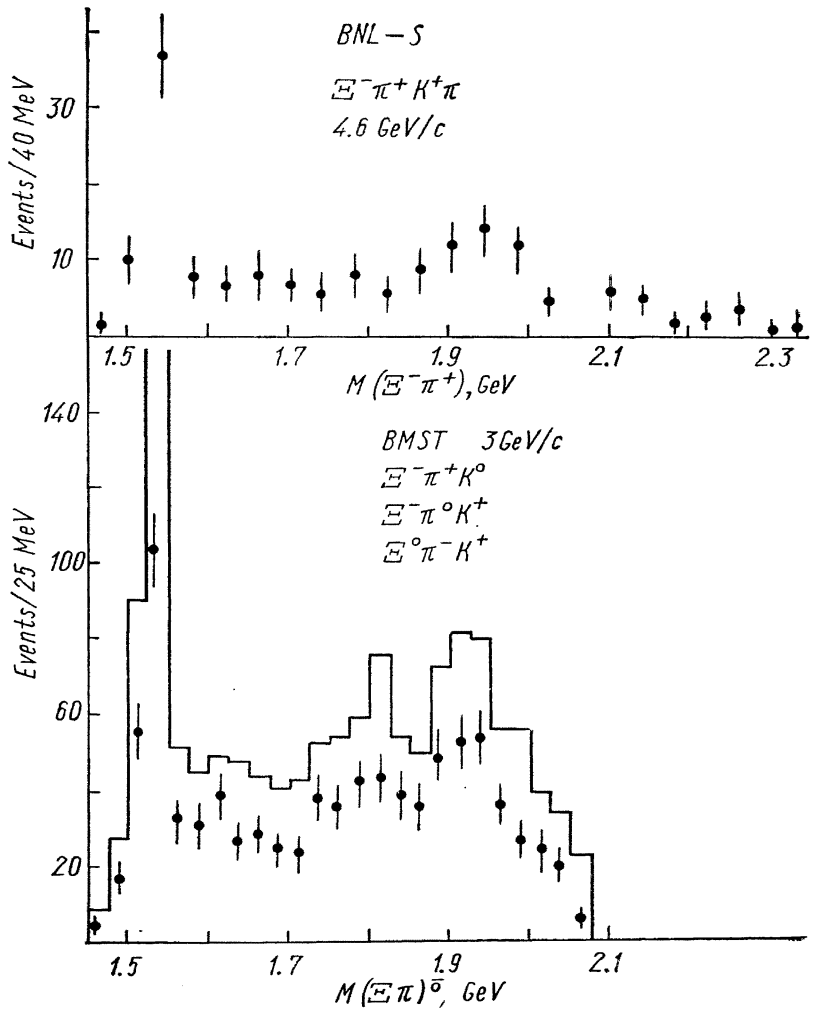

Fig. 18.

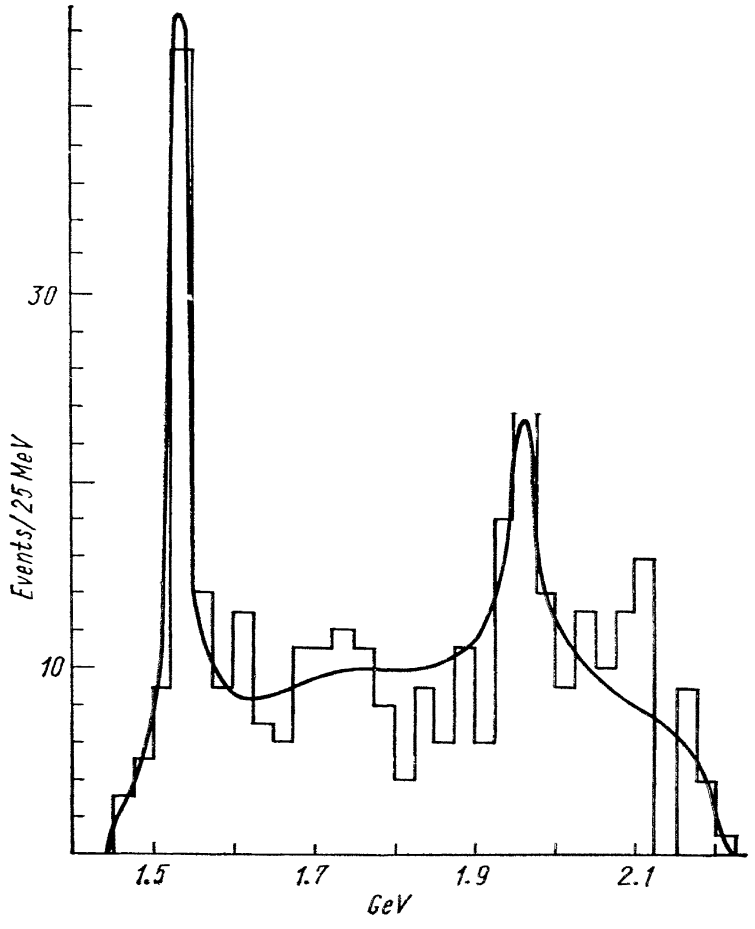

Fig. 19. $K^-p \to \Xi^0\pi^-K^+$; $K^-p \to \Xi^-\pi^0K^+$; 329 events. Oxford. $(\Xi\pi)^-$ mass.

effect is somewhat reduced in the sample without K (890). The Oxford bubble chamber group [37] has also reported experimental evidence (at this Conference) for the Ξ (1930) produced at 3.2 *GeV/c*. Their data are shown in Fig. 19. Their observed width is 35 ± 12 *MeV*, slightly smaller than the previously reported value of 80 *MeV*. In addition, new information was conveyed to the Conference by the Ecole Polytechnic — Saclay [38] collaboration studying K^-p interactions at 3.95 *GeV/c*. This involved evidence for a broad Ξ (1820) and also for a Ξ (1950). By restricting themselves to Ξπ, Ξππ, etc. masses recoiling against a $K\pi$ system, they claim that the Ξ (1800) is composed of two parts, Ξ (1762) and Ξ (1838) both with width ≈ 50 *MeV*. As in the case of most Ξ states, the statistics are limited. However, in this instance, there is the added difficulty of assessing the contribution of the multichannel background and therefore of estimating the significance of the above. The Ξ situation is summarized in Table VIII where the reported states have been separated into three categories: 1) well established, 2) reasonable — those resonances observed by one or more groups, and 3) proposed but not confirmed. It is of course still an open question as to whether the Ξ (1820) is composed of one or more states. The Ξ (1635) has the difficulty of being less significant when the K (890) events are removed and of its not being seen at lower or higher energies, 2.7 *GeV/c* and 3.2 *GeV/c* (with more limited statistics), than it's observance at 2.9 *GeV/c*. There is no confirmation of the Ξ (2240) originally reported by the ABCLV collaboration [39]. The isospin for all the states in category 1) and 2) is well known to be $^1/_2$ with the J^P being unknown except for 1320 and 1530 resonances.

The final topic concerning Ξ states which I would like to discuss is that of the Ξ (1530) width. The best previous measurement has been that of UCLA [40] performed in 1963 which gave a value Γ = 7 ± 2 *MeV*. There are now three new numbers: Ecole Polytechnic — Saclay 3.9 *GeV/c*, Γ = 11 ± 2 *MeV*, resolution ≈ 4 *MeV*; BMST 2.9 *GeV/c*, Γ = 7 ± 3 *MeV*, resolution ≈ 10 *MeV*; BNL 4.6 *GeV/c*, Γ = 11 ± 2.5 *MeV*, resolution ≈ 3 *MeV*. In addition, I have recalculated the width from the published UCLA data, using their histogram and quoted resolution, and I obtain a value of 10 ± 2 *MeV*. The Ecole data are shown in

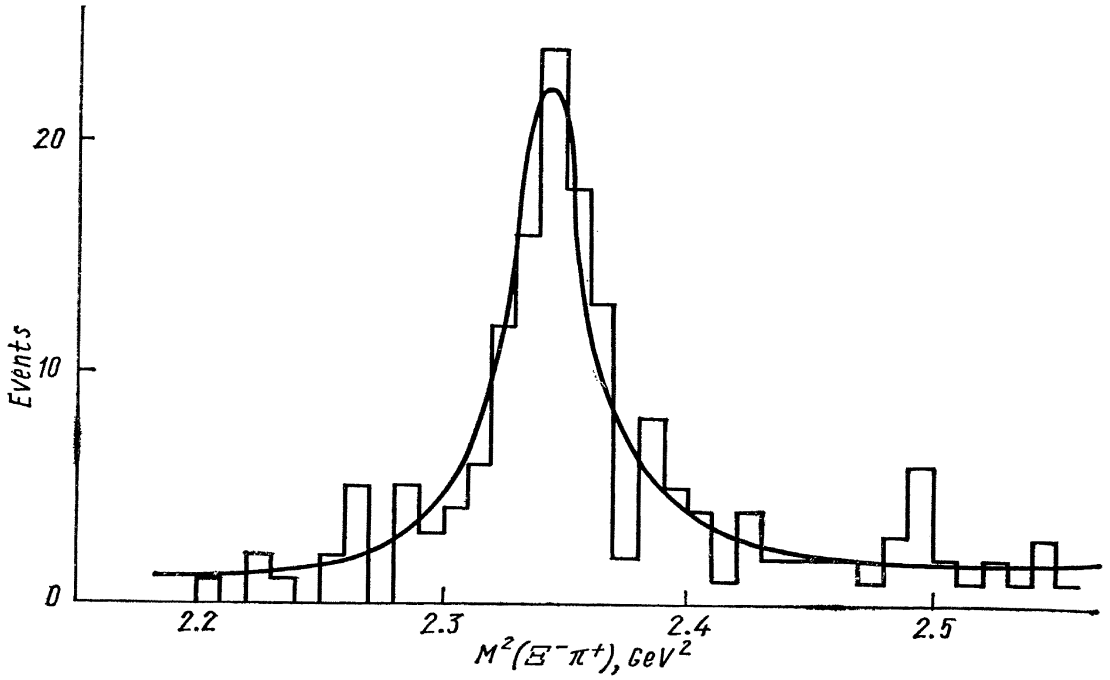

Fig. 20. Mass and width of Ξ* (1530). Ecole — Polytechnique, CEN — Saclay. The smooth curve is a maximum likelihood adjustment.

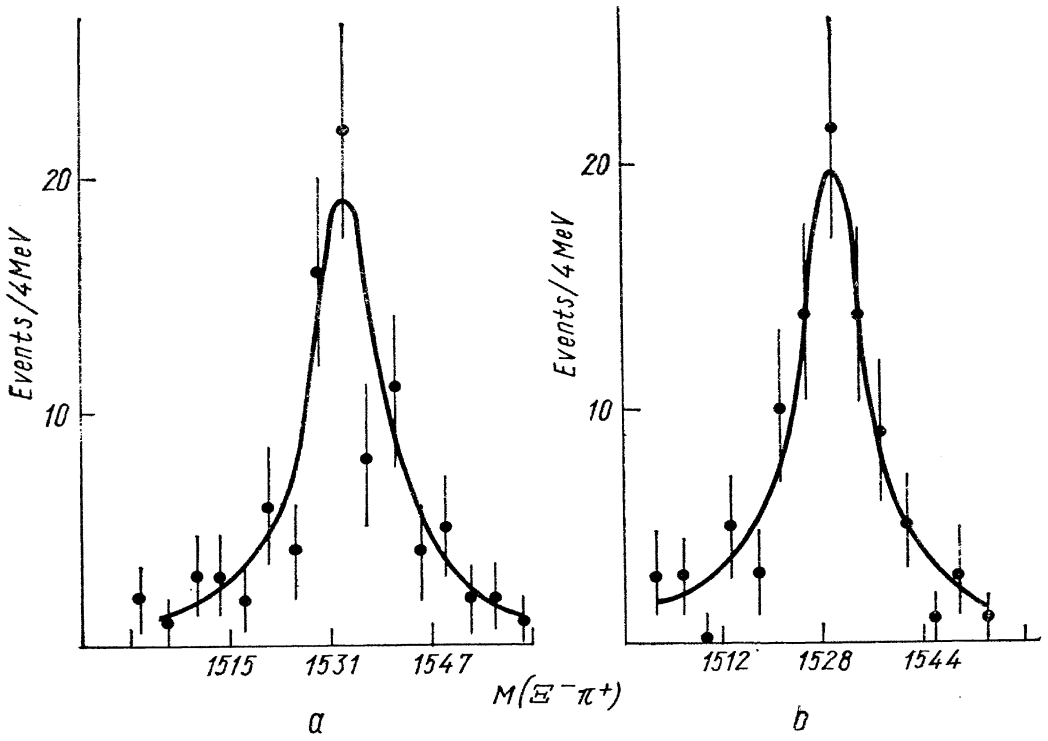

Fig. 21. (*a*) BNL. $K^-p \to \Xi^-\pi^+K^-\pi^+$; 91 events. $M = 1533 \pm 1$ *MeV*, $\Gamma = 11 \pm 2.5$ *MeV*. (*b*) UCLA. $K^-p \to \Xi^-\pi^+K^0$, 95 events.

Fig. 20 and that of BNL and UCLA in Fig. 21 with curves corresponding to the above widths. It is clear that the Ξ (1530) width is larger than the previously accepted 7 *MeV* and closer to 10 *MeV*. This is quite significant, as we shall soon see, concerning the *SU* (3) particle systematics.

4. Particle Systematics

With such an accumulation of data, a significant fraction of which is on firm footing, it is worthwhile to re-examine the success or failure of *SU* (3) as applied to this data. This has been an activity with many practitioners among which have been: Goldberg, Leitner, and O'Raferleigh [41], Tripp [42], Levi — Setti [43], and more recently the CHS collaboration [44] and Flaminio, Goldberg, Metzer, and myself [45]. The procedures adopted are slightly different and divide themselves as to whether one is formation or production experiment oriented. As noted earlier, different quantities are measured in these two types of experiments. In particular, in formation experiments one determines the amplitudes which are proportional to the square root of the product of the decay branching fractions while production experiments measure the branching fractions themselves. Similarly, Ξ states are not accessible to formation experiments and as a result such available information is not utilized in some analysis while every crumb is fed in by the alternate approaches. I have listed the more reputable Λ, Σ, Ξ, and lone Ω states as well as some of the N, Δ states reported by Dr. R.Plano in the previous talk in Table IX. One notes several N, Λ, Σ, Ξ resonances with the same J^P and even more numerous such $N\Lambda\Sigma$ combinations. One can either ignore the unknown $J^P\Xi$ states or assign them to a particular multiplet on the basis of the Gell-Mann — Okubo mass formula. Such an assignment is indicated in parenthesis next to each particular resonance. The general procedure is then outlined in Table X. It is essentially an unbroken *SU* (3) approach where

Table IX

N	Δ	Λ	Σ	Ξ	Ω
939 $1/2^+$					
		1115 $1/2^+$	1190 $1/2^+$		
	1238 $3/2^+$				
1518 $3/2^-$		1405 $1/2^-$	1385 $3/2^+$	1320 $1/2^+$	
1530 $1/2^-$		1520 $3/2^-$		1530 $3/2^+$	
1680 $5/2^-$		1670 $1/2^-$	1660 $3/2^-$		
1688 $5/2^+$		1690 $3/2^-$	1660 $3/2^-$		1672 $(3/2^+)$
			1765 $5/2^-$		
		1815 $5/2^+$			
		1830 $5/2^-$		1820 $(3/2^-)$	
	1950 $7/2^+$		1915 $5/2^+$	1930 $(5/2^-)$	
			2030 $7/2^+$	2030 $(5/2^+)$	
2190 $7/2^-$		2100 $7/2^-$			
			2280 $(7/2^-)$		
				2430 $(7/2^-)$	

Table X

SU (3)

Gell-Mann — Okubo

Octet, $\frac{m_N + m_\Xi}{2} = \frac{3m_\Lambda + m_\Sigma}{4}$; Decimet, Equal Spacing

Rates: $x \to yz$

$$\Gamma_i = \left|g^x_{yz}\right|^2 P_i^{2l}\left(\frac{P_i}{M_R}\right)$$

$\to$ Phase Space

$\to$ Barrier Factor

$\to$ SU (3) Factor

8→88

$$g^{x=m_8^P}_{yz} = \{-c_1 g_1 \sin\theta + (c_s g_s + c_a g_a)\cos\theta\}$$

$$g^{x=m_1^P}_{yz} = \{c_1 g_1 \cos\theta + (c_s g_s + c_a g_a)\sin\theta\}$$

$$g^{\text{others}}_{yz} = (c_s g_s + c_a g_a)$$

10 → 88

$$g = c_{10} g_{10}$$

Unknowns

Decimet: $10 \to 88$ g_{10}

Octet: $8 \to 88$ $g_s g_a$

Nonet: $g_1 g_s g_a$

Formation Experiments

$$t = \sqrt{\frac{\Gamma_e}{\Gamma}\cdot\frac{\Gamma_i}{\Gamma}}$$

$$t = \frac{g_e g_i}{\Gamma M_R}\left[P_e^{2l} P_i^{2l} P_e P_i\right]^{1/2}$$

$$\chi^2 = \Sigma\left(\frac{\Gamma_{SU(3)} - \Gamma_{exp}}{\Delta\Gamma_{exp}}\right)^2$$

any mass breaking is only taken into account via the phase space factor (P/M), M being the physical mass. The rate expression is not unique, however it is reasonable. The barrier term is given by P_i^{2l} where the radius factor R has been set equal to zero. The results are not sensitive to this choice of radius as long as it is small. The g coefficients contain the SU (3) isoscalar factors of de Swart [46] and the SU (3) invariant couplings. In the case of decimet or singlet decay into two octets, there is one unknown constant, g_{10} or g_1 respectively. For an octet decaying into two octets, there are two unknowns, g_s the symmetric and g_a antisymmetric couplings. In the most complex case, a singlet plus octet with mixing, there are three unknowns, g_s, g_a, and g_1, the mixing angle θ being determined from the mass formula and known masses. As noted earlier, formation experiments measure the amplitude t which in turn is proportional to the product of g factors. Fitting this amplitude directly has the advantage of avoiding depen-

Table XI

		Flaminio et al.			CERN—Heidelberg — Saclay		
J^P		α	θ	$\chi^2/d.f.$	α	θ	$\chi^2/d.f.$
$1/2^+$	8	.6—.7	—	—	—		—
$3/2^-$	9	.3	23°	.5	.31	25±6	.2
$5/2^+$	8	.4	—	.3	.55	—	.3
$7/2^-$	9	.1	23°	1.	—	—	—
$1/2^-$	9	1.2	20°	1.	—.53	18±17	1.2
$3/2^+$	10	—	—	.3	—	—	2.1
$5/2^-$	8	1.15	—	1.	1.24	—	.5
$7/2^+$	10?	—	—	1.	—	—	.7

$$\alpha = \left[1 + \frac{\sqrt{5}\, g_{a,f}}{3\, g_{s,d}}\right]^{-1}$$

ding on an accurate knowledge of Γ_e/Γ, poorly known in many cases. In production experiments the total widths and branching fractions are measured, thereby yielding the partial rates directly. The parameters are varied such as to minimize the χ^2 formed from the experimental SU (3) predicted partial rates or amplitudes. With the increased data, both in accuracy and magnitude, the properties of several well-known SU (3) families have been enhanced as well as uncovering two new possibilities. In particular, the $J^P = 3/2^-$ nonet [N (1518), Λ (1520), Λ (1695), Σ (1660), Ξ (1820)]; $5/2^+$ octet [N (1688), Λ (1815), Σ (1915), Ξ (2030)]; and $5/2^-$ [N (1680), Λ (1830), Σ (1765), Ξ (1930)] fit the SU (3) pattern rather well. Detailed information concerning these multiplets will not be repeated since they have not radically changed since the last Conference at Vienna. The χ^2 per degree of freedom, as derived by the two recent analyses, is shown in Table XI. Also included are the derived mixing angles θ and α and the ratio of the symmetric to the sum of the symmetric and antisymmetric couplings. The importance of mixig is graphically illustrated in Fig. 22 by the CHS fit where the g_D and g_F couplings are plotted for the various decay modes in the $3/2^-$ nonet. It is noted that without mixing there is no common intersection, while the introduction of 25° of mixing brings an excellent convergence. Although the $1/2^+$ octet fits the mass formula rather well, the situation with the $\Lambda\bar{K}N$, $\Sigma\bar{K}N$ coupling constants is not definitive. The extrapolation to the unphysical region of the experimental low energy KN data via the K-matrix formalism has a relatively large uncertainty. The $\Sigma\bar{K}N$ coupling constant is certainly small, <3, while the $\Lambda\bar{K}N$ can lie

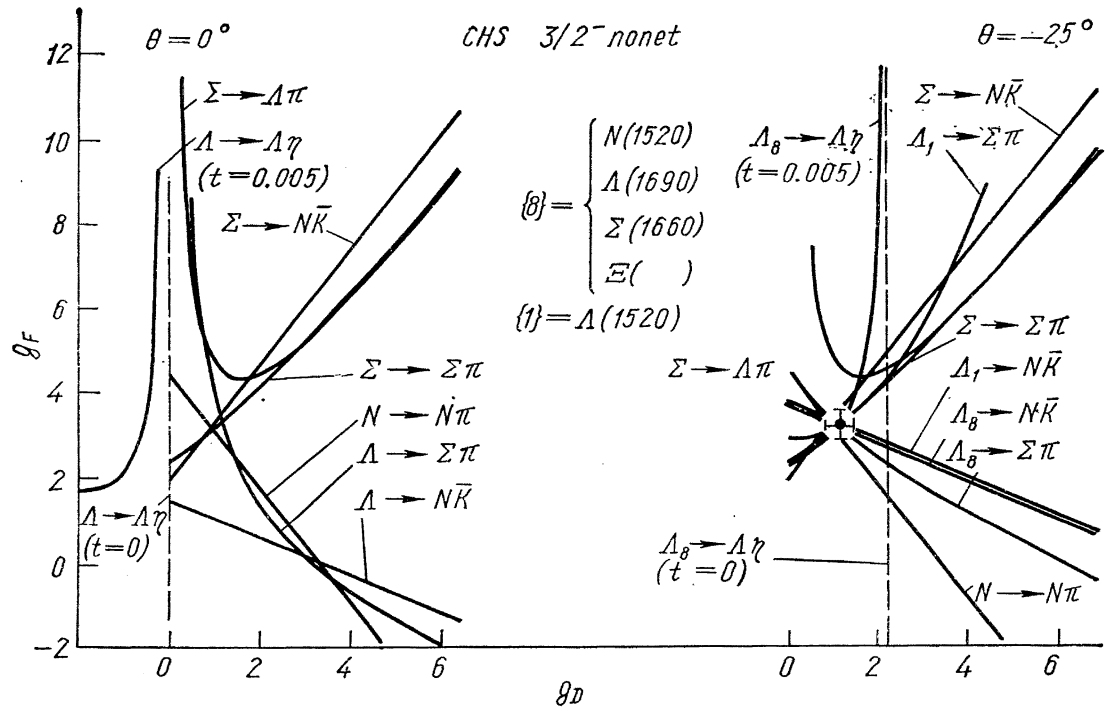

Fig. 22.

anywhere between 3 and 17. Additional information has recently been obtained from studying $\pi^- p$ charge exchange and ηN backward production, which however is model dependent. Although poorly known, all evidence indicates $\alpha = 0.6$—0.7.

The new evidence on the Ξ (1530) width indicates that it is broader, closer to 10 *MeV* than 7.5 *MeV* and removes the previous difficulty with the $3/2^+$ decimet. The relevant information is shown in Table XII listing the experimental

Table XII

	$J^P = 3/2^+$ Decimet	
$\Omega^-\Xi^-$	$\Xi^- - \Sigma^-$	$\Sigma^- - \Delta^-$
140±2.5 *MeV*	145.8±4.0 *MeV*	146.7±6.0 (*MeV*)
	Γ_{exp} (*MeV*)	$\Gamma_{SU(3)}$ (*MeV*)
Δ (1238) → πN	120±5	116
Σ (1385) → πΛ	33±6	37
→ πΣ	3.6±1.5	3.8
Ξ (1530) → πΞ	(7.5±3)	13
	10±3 New	
		$(\chi^2/d.f. = 9/3)$
		$\chi^2/d.f. = 1/3$

and *SU* (3) predicted rates. The χ^2 is reduced from 9 to 1 for 3 degrees of freedom. The equal mass spacing among the four members is well satisfied, the most accurate value occurring for the $\Omega^-\Sigma^-$ mass difference and the poorest for $\Sigma^-\Delta^-$. The possibility of two additional multiplets, $1/2^-$ and $7/2^-$ nonets, has recently received added weight. The experimental situation is reviewed in Table XIII. In the former $1/2^-$ nonet, the N (1525), Λ_1 (1405), and Λ_8 (1670) are well-established states while the Σ (1750) is controversial. The results of the *SU* (3) analysis require a mixing angle of $\approx 20°$ and a Ξ (1825) which is predicted to predominately decay via Ξπ mode. Such a possibility certainly exists, as mentioned under the Ξ discussion, although there is as of yet no convincing evidence for such a Ξ state. The greatest previous difficulty in the formulation of this nonet has been the N (1525) → $\pi N/\pi\eta$ branching ratio of $\approx {}^1/_2$ while the *SU* (3) fit prefers

a ratio $^{8}/_{1}$. The recent re-analysis of η production through the N (1525) mass region [47] has reduced the experimental N (1525) $\rightarrow N\eta$ partial rate by a factor of ≈ 5 removing this difficulty. As such, the χ^2 for this multiplet is now 2 for 6 degrees of freedom, quite satisfactory. In the case of the proposed $7/2^-$ nonet, the properties of the N (2190), Λ (2100), and Σ (2280) are well established with the existence of the Λ (2350) and Ξ (2430) on reasonable footing but not their J^P.

Table XIII

$J^P = 1/2^-$ Nonet

	Γ_{exp} (*MeV*)	$\Gamma_{SU(3)}$(*MeV*)
N (1525) $\rightarrow \pi N$	27 ± 19	24
$\rightarrow \eta N$	(52 ± 38)	3
	11 ± 7 New	
Λ_1 (1405) $\rightarrow \pi\Sigma$	38 ± 6	35
Λ_8 (1670) $\rightarrow \bar{K}N$	7 ± 4	10
$\rightarrow \pi\Sigma$	15 ± 6	10
$\rightarrow \eta\Lambda$	6 ± 3	4
Σ (1750) $\rightarrow \bar{K}N$	18 ± 10	29
$\rightarrow \pi\Lambda$	18 ± 10	15
$\rightarrow \eta\Sigma$	12 ± 21	5
Ξ (1825) $\rightarrow \pi\Xi$	—	33
$\rightarrow \bar{K}\Sigma$	—	6
$\rightarrow \bar{K}\Delta$	—	13

$|\theta| = 20°$
$\chi^2/d.f. = 2/6$

$J^P = 7/2^-$ Nonet

	Γ_{exptl} (*MeV*)	$\Gamma_{SU(3)}$(*MeV*)
N (2190) $\rightarrow \pi N$	60 ± 28	57
Λ (2100) $\rightarrow \bar{K}N$	35 ± 5	40
$\rightarrow \pi\Sigma$	16 ± 3	16
$\rightarrow \eta\Lambda$	4 ± 2	2
$?\Lambda_8$(2350) $\rightarrow \bar{K}N$	33 ± 8	33
$\rightarrow \pi\Sigma$	—	23
$\rightarrow \bar{K}\Xi$	—	17
Σ (2280) $\rightarrow \bar{K}N$	6 ± 20	19
$\rightarrow \pi\Sigma$	92 ± 32	59
$\rightarrow \pi\Lambda$	22 ± 20	2
Ξ (2430) $\rightarrow \bar{K}\Lambda$	75 ± 39	29
$\rightarrow \bar{K}\Sigma$	75 ± 39	25
$\rightarrow \pi\Xi$	—	6

$|\theta| = 23°$
$\chi^2/d.f. = 8/7$

Previous evidence favored $7/2^-$ for the Λ (2350) but the recent investigation of Bricman et al. [22] suggests $9/2^+$ as the most probable value. Further work is clearly needed. The spin parity of the Ξ (2430) is unknown. With these reservations, the observed partial widths are well reproduced by SU (3), $\chi^2 = 8$ for 7 degrees of freedom as noted in Table XIII. The preponderance of $\Lambda\bar{K}$, $\Sigma\bar{K}$ over $\Xi\pi$ decay of the Ξ (2430) and the strong $\bar{K}N$ coupling of the Λ (2100) are well reproduced. The strong $\pi\Sigma$ decay of the Λ (2350) should be sought as well as possibly its observable ΞK decay.

A summary of the relevant parities of all the discussed multiplets is noted in Table XI. Tle sequence $1/2^+$, $3/2^-$, $5/2^+$, $7/2^-$ has small values of α to be

contrasted with values of ≈ 1 for $1/2^-$ and $5/2^-$ multiplets. The pattern for α and θ certainly suggests that the higher multiplets are Regge recurrences of the lower spin-parity families; ($5/2^+$, $1/2^+$) octets, ($7/2^-$, $3/2^-$) nonets, and ($7/2^+$, $3/2^+$) decimets. The α values of 1.2 is similar for $5/2^-$ and $1/2^-$ multiplets, however only eight members have been uncovered with $J^P = 5/2^-$ while the $1/2^-$ multiplet is a nonet with $\theta = 20°$. If a similar mixing angle was assigned to the $5/2^-$ multiplet, one would then expect a Λ state at a mass of 1670 *MeV*. Such a fit has been performed by Flaminio et al. [45], the results of which improve the χ^2, as expected, and require that the conjectured new Λ state be strongly coupled to $\Sigma\pi$, 32 *MeV* partial width and more weakly coupled to $\bar{K}N$, 11 *MeV* partial width. The recurrence property discussed above is illustrated in the Chew — Frautschi plots of Figs. 23 and 24 where M^2 (mass squared) is plotted as a function of the J^P for these N, Δ, Σ, and Ξ states. The Λ's have been omitted due to their mass displacement caused by singlet-octet mixing. One notes that the trajectories are roughly parallel to one another with a slope ≈ 1. However, they are clearly not exchange degenerate, the lines being certainly displaced from one another.

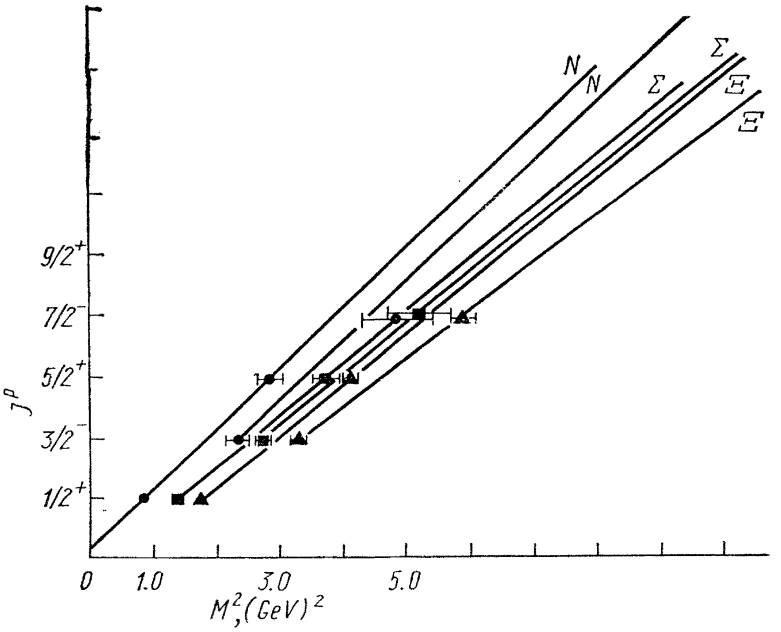

Fig. 23.

One final comment is in order before completing this discussion of *SU* (3) particle systematics. This involves the analysis of *S* channel resonance interference effects as originally suggested by Kernan and Smart[48]. The application of this technique has been used extensively and the results summarized by Levi — Setti in his clock figure at Lund[43]. The main results have arisen from the observation of interferences between a member of a decimet and a singlet or octet. In particular, the Λ(1405) and Λ (1520) each interfering with the Σ (1385) have been shown to be mainly members of a singlet and not octet representation. Other investigations have involved the interferences with the Σ (2030) and numerous other states, the results of which rely on the Σ (2030) being a member of a decimet, this being an assumption since this has yet to be demonstrated. The effectiveness of the technique to octets has been minimal and even misleading. This is due to the fact that in this instance

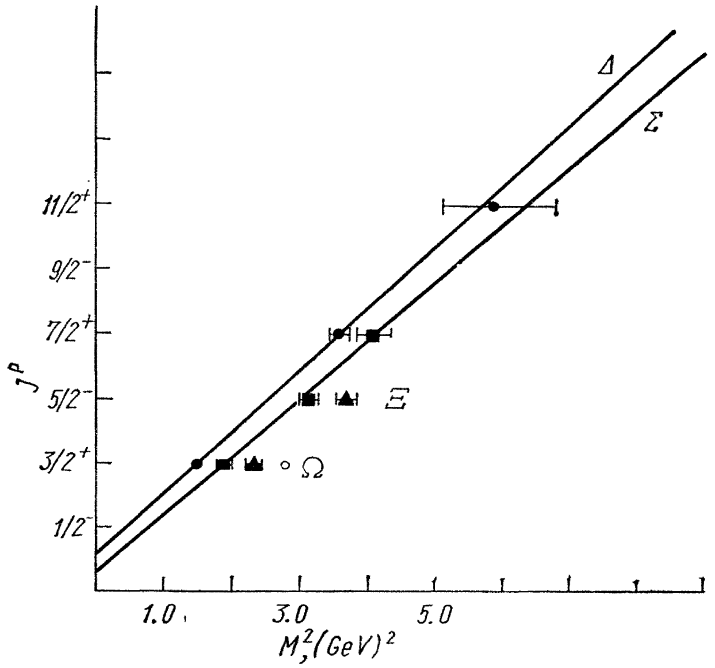

Fig. 24.

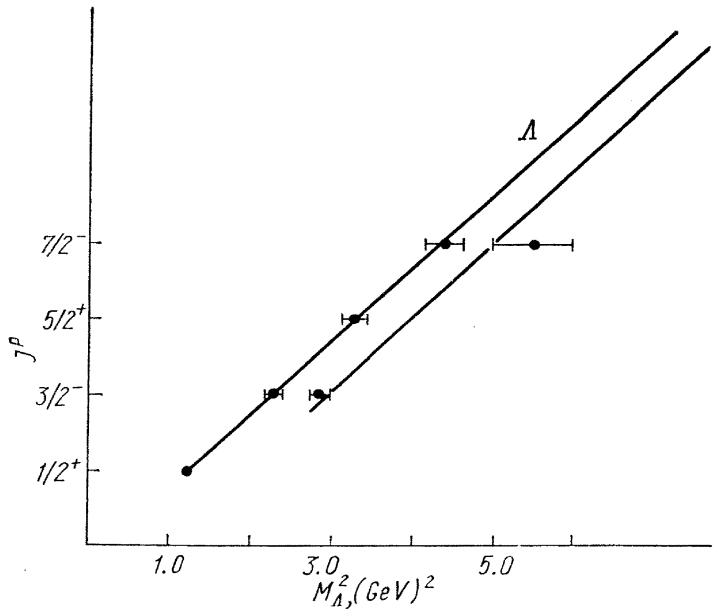

Fig. 25.

the sign of the interference is dependent on the α parameter in the form $(1 - 2\alpha)$ [for Σ production by $\bar{K}N$ interaction]. As such, the sign will change as to whether $\alpha = 0.5 + \varepsilon$ or $0.5 - \varepsilon$ where ε is a small number. This is precisely the case in the $5/2^+$ octet where some difficulties have been encountered. Such an analysis is simply not applicable in this instance, especially in view of the fact that some symmetry breaking is known to occur which also could alter the sign of the interference. In essence, this technique has proved extremely useful in a limited number of cases, but should be handled with caution in others.

One can summarize the major conclusions for strange baryons as follows:

1. There are many well-established *SU* (3) families, octets, nonets, and decimets which also display Regge regularities.
2. The properties of numerous resonances have been determined and many additional Λ, Σ, and Ξ states have been reported, many of these with relatively low mass and low spin-parity values. In addition, there is the interesting possibility of the existence of two Σ (1660) states with the same spin parity, $3/2^-$.
3. The question of the existence of Z^* states is still unresolved. There are now three such candidates, the newest Z_0 (1780) probably being the most likely area to yield a definitive answer since it is mainly elastic.

All in all, the knowledge of the detailed spectra keeps increasing at a rapid rate. With the many additionally conjectured states, it may be that only the surface of a large number of low lying states is being observed and that the situation is much more complex than previously realized. Hopefully, intensive work over the next years will help in resolving the present problems and clarifying the overall picture.

Note added in proof: The Chew — Frautschi plot for the Λ resonances is displayed in Fig. 25 for the $1/2^+$, $3/2^-$, $5/2^+$, $7/2^-$ sequences. There are two states plotted for the $3/2^-$, $7/2^-$ multiplets since these are nonets, the lower mass being essentially a member of a singlet and the higher mass an octet representation. The trajectories connecting the respective Λ octet members are roughly parallel with that connecting $(1/2^+, 5/2^+)$ being exchange degenerate with the singlet $(3/2^-, 7/2^-)$, the slopes being ≈ 1.

DISCUSSION

B i n g h a m:

Evidence for a Ξ^* state with mass about 1770 *MeV* decaying to $\Xi\pi\pi$ was presented at the 1963 Vienna conference. The data were obtained with the CERN HLBC, K^- of 3.5 *GeV/c*, analyzed by Bergen — CERN — Ecole — Polytechnique — University College London collaboration as a by-product of an unsuccessful Omega minus hunt.

Y o k o s a w a:

I have a comment on determining whether there exists a Z^* resonance or not. It seems to me that a speed plot shown is a confusing one especially when a partial wave consists of background and resonance terms. I think that one should fit the partial wave in terms of a resonance and background and then if we find in that fit a constant background or smoothly varying background, one should recognize the existence of a resonance.

L i p k i n:

You have not considered the SU (6) or quark model classifications of these states. If there are negative parity decimets, as predicted by these models, they would change the picture considerably, and there could be octet-decimet mixing in the sigmas and cascades. The existence of negative parity Δ's indicates the existence of negative parity decimets, and you cannot pretend they are not there and just fit the rest of the data.

S a m i o s:

The question of the reliability of the existence of negative parity Δ states should be directed to Prof. Plano. Concerning Σ resonances, the only decimet candidates are positive parity states. With regard to other designation schemes such as SU (6), I have purposely restricted myself to the SU (3) classification because the options for other schemes are innumerable due to insufficient accuracy and extent of the data as to make such an examination not too meaningful. As a result the approach has been to utilize the more reliable data in considering SU (3) multiplets, which in turn can be used, when more SU (3) families are uncovered, to construct SU (6) or other multiplets. Finally with respect to octet-octet and octet-decimet mixing, both can of course occur. It has not been necessary to introduce such a mixing since the present spectra can be fit without introducing further parameters.

B a l u n i:

Have you found any regular dependence of the width on the mass?

S a m i o s:

No.

S c h m i d:

A comment about your last slide: Some baryon trajectories are expected to be exchange degenerate, others are expected not to be. The $\Lambda\left(\frac{1}{2}^+\right) - \Lambda\left(\frac{3}{2}^-\right)$ trajectories and the $\Sigma\left(\frac{3}{2}^+\right) - \Sigma\left(\frac{5}{2}^-\right)$ trajectories couple strongly to $\bar{K}N \to \bar{K}N$, i. e. to a channel whose crossed channel ($KN \to KN$) is exotic. Therefore we expect an exchange degeneracy, and indeed it is observed experimentally. A particularly beautiful sequence is $\Lambda\left(\frac{1}{2}^+, \frac{3}{2}^-, \frac{5}{2}^+, \frac{7}{2}^-, \frac{9}{2}^+?\right)$. On the other hand the $N\left(\frac{1}{2}^+\right)$ and $N\left(\frac{3}{2}^-\right)$ trajectories couple strongly to $\pi N - \pi N$, i. e. to a channel whose crossed channels are not exotic. Therefore we expect not to see an exchange degeneracy, and indeed it is not observed experimentally. Similarly the $\Sigma\left(\frac{1}{2}^+\right)$ and $\Sigma\left(\frac{3}{2}^-\right)$ trajectories couple only very weakly to $\bar{K}N - \bar{K}N$, where the crossed channel is exotic, therefore we have no reason to expect the exchange degeneracy for these trajectories.

C a p p s:

There is some ambiguity, I believe in the α value of the $\frac{5}{2}^+$ octet. The sign of the resonant $\bar{K}N \to \pi\Sigma$ amplitude tells whether α is less or greater than $\frac{1}{2}$. The Berkeley people can correct me if I'm wrong. But I believe their measurement indicates $\alpha > \frac{1}{2}$, whereas your branching ratio analysis indicates $\alpha < \frac{1}{2}$. This is interesting because the $\frac{5}{2}^+$ octet is the Regge recurrance of the nucleon octet, where $\alpha > \frac{1}{2}$.

REFERENCES

1. Hyperon Resonances — 70 (Proc. Conf. held at Duke University, April 24—25, 1970) (North Carolina: Moore Publishing Co., 1970).
2. M. Gell-Mann, Phys. Letters **8**, 214 (1964).
3. G. Zweig, CERN Report 8419/TH. 412 (1964) (unpublished).
4. R. L. Cool et al., Phys. Rev. Letters **16**, 1228 (1966); Phys. Rev. Letters **17**, 102 (1966).
5. D. V. Bugg et al., Phys. Rev. **168**, 1466 (1968).
6. R. J. Abrams et al., Phys. Letters **30B**, 564 (1969).
7. F. C. Erne et al., paper 6—16.
8. G. A. Rebka et al., Phys. Rev. Letters **24**, 160 (1970); Pres. at XVth Intern. Conf. on High Energy Physics, Kiev, USSR, Aug. 26 — Sept. 4, 1970.
9. S. Kato et al., Phys. Rev. Letters **24**, 615 (1970); paper 6—3.
10. G. Goldhaber, Hyperon Resonances — 70 (Proc. Conf. held at Duke University, April 24—25, 1970) (North Carolina: Moore Publishing Co., 1970), p. 407.
11. R. W. Bland et al., Phys. Letters **29B**, 618 (1969).
12. B. Carreras and A. Donnachie, contribution to this conference.
13. R. Ayed et al., Phys. Letters **32B**, 404 (1970).
14. A. Hirata et al., Phys. Rev. Letters **21**, 1728 (1968).
15. D. V. Bugg, Phys. Rev. **168**, 1466 (1968).
16. T. Bowen et al., Hyperon Resonances — 70 (Proc. Conf. held at Duke University, April 24—25, 1970) (North Carolina: Moore Publishing Co., 1970), p. 3.
17. R. J. Abrams et al., Phys. Letters **30B**, 564 (1969).
18. G. Lynch, Hyperon Resonances — 70 (Proc. Conf. held at Duke University, April 24—25, 1970) (Notrh Carolina: Moore Publishing Co., 1970), p. 9.
19. J. K. Kim, Phys. Rev. Letters **19**, 1074 (1967); Hyperon Resonances — 70 (Proc. Conf. held at Duke University, April 24—25, 1970) (North Carolina: Moore Publishing Co., 1970), p. 161; paper 6—7.
20. R. Dalitz and S. Tuan, Ann. Phys. (NY) **10**, 307 (1960).
21. M. Ross and G. Shaw, Ann. Phys. (NY) **13**, 147 (1961).
22. C. Bricman et al., Phys. Letters **31B**, 152 (1970).
23. CRS (College de France, Rutherford High Energy Laboratory, CEN — Saclay) Reports presented at the Gonf. held at Duke University, April 24—25, 1970 and paper 6—8.
24. R. P. Ely et al., paper 6—14.
25. V. E. Barnes et al., Phys. Rev. Letters **22**, 479 (1969).
26. P. Eberhard et al., Phys. Rev. Letters **22**, 200 (1969).
27. M. Aguilar-Benitez et al., Phys. Rev. Letters **25**, 58 (1970).
28. M. Derrick et al., Phys. Rev. Letters **18**, 266 (1967); D. C. Colley et al., Phys. Letters **24B**, 489 (1967).
29. D. J. Crennell et al., Phys. Rev. Letters **21**, 648 (1968).
30. R. Barloutaud et al., Nuc. Phys. **B16**, 201 (1970).
31. B. A. Shahbazian and A. A. Timonina, paper 6—10.
32. G. A. Smith et al., Phys. Rev. Letters **14**, 25 (1965).
33. Brandeis, Maryland, Syracuse, Tufts collaboration.
34. J. Alitti et al., Phys. Rev. Letters **22**, 79 (1969); contribution to this conference.
35. J. Badier et al., Phys. Letters **16**, 171 (1965).
36. G. A. Smith and J. S. Lindsey, Proc. of the Second Topical Conf. on Resonance Particles, Athens, Ohio (1965), p. 251.
37. Oxford Bubble Chamber Group, paper 6—15.
38. Ecole Polytechnic, CEN — Saclay, paper 6—6.
39. Aachen, Berlin, CERN, London, Vienna collaboration, Phys. Letters **28B**, 439 (1969).
40. P. Schlein et al., Phys. Rev. Letters **11**, 167 (1963).
41. M. Goldberg et al., Il Nuovo Cimento **45A**, 169 (1966).
42. R. D. Tripp et al., Nucl. Phys. **B3**, 10 (1967); Proc. 14th Intern. Conf. on High Energy Physics, Vienna (1968), p. 173.
43. R. Levi — Setti, Proc. Lund Intern. Conf. on Elementary Particles, Lund, (1969), p. 339.
44. D. E. Plano et al., (to be published in Nuc. Phys.).
45. E. Flaminio et al., BNL Report 14572.
46. J. J. de Swart, Rev. of Mod. Phys. **35**, 916 (1963).
47. N. T. Diem et al., contribution to this conference.
48. A. Kernan and W. Smart, Phys. Rev. Letters **17**, 832 (1966).